Reviews of Scientific Papers on

Fuzzy Shape Analysis

Nataša Sladoje

Winter 2003/2004

Foreword

The intention of this report is to list and analyze some of the published results related to different approaches of applying fuzzy set theory to fuzzy shape analysis. These results provide a good background for further development of fuzzy shape analysis methods, which is our main goal.

It should be noted that only fuzzy shape analysis techniques are considered, and not other approaches to use fuzzy set theory in (crisp) shape analysis (like, e.g., fuzzy reasoning). Even the methods referring to grey-level images are studied only if their adjustment to fuzzy sets is straightforward, by simple normalization of grey levels to the interval $[0, 1]$. The focus is, thus, on the shapes obtained by segmentation techniques which assign to the image pixels application-dependent membership values to the fuzzy object (shape).

The overall organization of the paper is as follows: At the beginning (Section 1) a brief introduction is given. It refers to the classification and evaluation of existing crisp shape analysis methods, as well as to the general approaches when introducing fuzziness into the binary concepts. Section 2 introduces some basic fuzzy shape definitions. In Sections 3 and 4, we report on a class of shape analysis methods which produce a numerical shape descriptor, such as extent, diameter, area, perimeter, shape signature, Fourier transform based motion descriptor, and moments. Sections 5 is related to shape descriptors which produce an image (non-numerical result) as an output; we report on convexity, symmetry, distance transform, medial axis transform, and mathematical morphology, in fuzzy settings. Section 6 contains some comments on the reported results. The reporting style balances between "easy to follow" and "get the information" concept; we would be very glad if both, rather than none, is achieved.

Contents

1 Introduction

1.1 Shape analysis for binary images

The shape of an object is an image representing the extent of an object; it can be thought of as a silhouette of the object. It is often referred to as a region. There are many imaging applications where image analysis can be reduced to the analysis of shapes, in contrast to texture analysis. Examples are images of, e.g., organs, cells, machine parts, characters, etc.

There exist different classifications of shape analysis techniques, see, e.g., [21] for an overview. Depending on if only the shape boundary points are used for the description, or alternatively, the whole interior of a shape is used, the two resulting classes of algorithms are known as boundary-based (external) and region-based (internal), respectively. Examples of the former class are the algorithms which parse the shape boundary and various Fourier transforms of the boundary. They are used when the primary focus is on the shape characteristics. The internal representations are selected when the primary focus is on the regional properties, and region-based methods include,for example, the medial (symmetric) axis transform, moment-based approaches, and methods of shape decomposition into the primitive parts.

A *description* of a shape is data representing it in a way which is suitable for further computer processing. Such data can be low-dimensional, like, e.g., perimeter, or moments, or high-dimensional, such as, e.g., medial axis or primitive parts. The first type of data is suitable for, e.g., shape classification, while the second, often called shape *representation*, provides, e.g., good visual interpretation and compression.

A resulting classification scheme for the shape analysis methods may look as follows:

Boundary based numeric methods result in a numerical description based on shape boundary points. Examples of this approach are chain-code and perimeter, but also one-dimensional functions constructed from the two-dimensional shape boundary, called shape signatures. In that case, the shape is described indirectly by means of a one-dimensional characteristic function of the boundary, instead of the two dimensional boundary itself. The Fourier transform is often applied to the signature functions, and used as a shape descriptor.

Boundary based non-scalar methods take shape boundary as input and produce the result in pictorial or graph form. Examples are boundary approximations by polygons and splines, and boundary decomposition.

Region-based numeric methods compute scalar result(s) based on the global shape. Moment-based methods are popular example from this group. Area and compactness measures are also often used, although not information-preserving.

Region-based non-numeric methods result in a spatial representation of a shape, based on the whole shape's interior. The most popular methods in this group are medial axis transform and shape decomposition. Mathematical morphology, suitable for shape-related processing since morphological operations are directly related to object shape, is

in this group of approaches as well.

The goal of a shape description is to uniquely characterize the shape. The required properties of a shape description scheme are invariance to translation, scale, and rotation; these three transformations, by definition, do not change the shape of an object, and consequently should not change its descriptor. However, it should be noted that in the discrete case such invariance exists only up to discretization effects.

Additional desired properties of a good shape description method are

- accessibility – How easy is it to compute a descriptor in terms of memory requirements and computational time; are the operations local, or global?
- scope – How wide is the class of shapes that can be described by the method?
- uniqueness – Is there a one-to-one mapping between the set of shapes and the set of shape descriptors?
- stability and sensitivity – How sensitive is a shape descriptor to small changes of a shape?

1.2 Membership functions and fuzzification principles

Fuzzy membership of a point reflects the level to which that point fulfills certain criteria to be a member of a set. A specific fuzzy membership function defining the observed fuzzy set depends on a specific problem to be solved. The only theoretical requirement for a membership function is to be a function into $[0, 1]$, but in practice, the underlying interpretation plays an important role when designing a function. Values 0 and 1 have a special role, expressing certainty, while the importance of 0.5 membership value is related to its common use as a decision threshold.

Even though the segmentation results obtained by binarization (defuzzification) of a fuzzy segmented image are improved compared to those obtained by classical binary segmentation methods (see, e.g., [45]), and thus provide a good start for any further classical image analysis procedure, it has become clear that the segmentation should not be the only step in the image analysis process where inaccuracy of the data is to be considered; information-rich inherent fuzziness of the image, which is lost after the defuzzification, should instead be exploited further in the process. Shape analysis is often the next step in the image analysis process, so naturally it is the next step to carry the fuzziness to.

There are three main representations of a fuzzy set F defined on a reference set X, [16]:

- membership function $\mu_F : X \to [0, 1]$ which assigns to each $x \in X$ its membership grade $\mu_F(x)$ to the fuzzy set F;
- set of α-cuts $C(F) = \{F_\alpha \mid \alpha \in [0, 1]\}$ of the set F, where $F_\alpha = \{x \mid \mu_F \geq \alpha\}$;

- convex combination of sets, i.e., a pair (F, m), where a positive weight m, is attached to each element A of F, and
$$\sum_{A \in \mathcal{F}} m(A) = 1.$$
The weights m are called basic probability assignment, and $A \in F$ a focal subset. (F, m) can be called a random set, and $m(A)$ is the probability that A is the "true" representative of (F, m).

There exists a correspondence between different interpretations of a fuzzy set. The fuzzification principle, based on understanding of a fuzzy set as a stack of its α-cuts, uses one of the following equations

$$F(\mu) = \int_0^1 \hat{F}(\mu_\alpha) d\alpha, \quad (1)$$
$$F(\mu) = \sup_{\alpha \in (0,1]} [\alpha \hat{F}(\mu_\alpha)] \quad (2)$$

to fuzzify a binary function $\hat{F}$. Note that various properties defined for binary sets in the stack can be generalized and derived for a fuzzy set, including the membership function, itself (from the characteristic function of the α-cuts).

A membership function μ_F can be obtained from a convex combination of characteristic functions μ_A of sets A in F as:

$$\mu_F(x) = \sum_{A \subseteq X} m(A) \mu_A(x) = \sum_{A \in F, x \in A} m(A). \quad (3)$$

In order to provide a unique correspondence between the random set and the membership function, only the nested family F of sets $\{A_1 \subseteq A_2 \subseteq \ldots \subseteq A_n\}$ is observed. Let $M(F) = \{\alpha_1 > \alpha_2 > \ldots > \alpha_n\}$ be the set of positive membership grades for F. The random set such that (3) holds is defined by

$$F = \{F_{\alpha_1} \subseteq F_{\alpha_2} \subseteq \ldots \subseteq F_{\alpha_n}\}$$

and for each A

$$m(A) = \begin{cases} \alpha_i - \alpha_{i+1}, & \text{if } A = F_{\alpha_i} \\ 0, & \text{otherwise} \end{cases},$$

with the convention $\alpha_{m+1} = 0$.

In other words, the focal sets are the α-cuts, and for $x \in F_{\alpha_i}$ such that $x \notin F_{\alpha_{i-1}}$

$$\mu_F(x) = \sum_{j=i,n} m(F_{\alpha_j}).$$

The described representations and connection between them provide one way to extend binary concepts to the case of fuzzy sets. The other approach to derive fuzzy definitions

from the crisp ones is to translate binary set theoretical and logical operations and relations into their fuzzy equivalents. After replacing a set by a membership function, negation (set complement), conjunction (set intersection), and implication (set inclusion) can be fuzzified by using operators called, respectively, negator, conjunctor, and implicator [23]:

Negator is a unary operator on the interval $[0, 1]$, which coincides with the Boolean negation on $\{0, 1\}$, and is a decreasing and involutive mapping; the standard one is defined by $\mathcal{N}(x) = 1 - x$;

Conjunctor is a binary operator on the interval $[0, 1]$, which coincides with the Boolean conjunction on $\{0, 1\}^2$, and is an increasing mapping in each variable; in addition, for each $x \in [0, 1]$ it holds that $\mathcal{C}(1, x) = \mathcal{C}(x, 1) = x$, and is commutative and associative. An operator with these properties is called t-norm; the standard ones are defined by $\mathcal{C}(x, y) = \min\{x, y\}$ or $\mathcal{C}(x, y) = x \cdot y$.

Implicator is a binary operator on the interval $[0, 1]$, which coincides with the Boolean implication on $\{0, 1\}^2$, and is a decreasing mapping in first, and an increasing mapping in second variable; in addition, for each $x \in [0, 1]$ it holds that $\mathcal{T}(1, x) = x$. The standard ones are defined by $\mathcal{T}(x, y) = \min\{1, 1-x+y\}$, or $\mathcal{T}(x, y) = \max\{1-x, y\}$.

Other set theoretic operations are easily derived from the ones listed above.

1.3 Fuzzy segmentation

The process of converting the input image into a fuzzy set by indicating, for each pixel, the degree of membership to the object, is referred to as "fuzzy segmentation". For a brief overview of fuzzy segmentation methods, see [40].

In the same way as it is convenient to model binary images as crisp sets, it is possible to model grey-level images directly as fuzzy sets. If the grey-level values of an image are scaled to be between 0 and 1, the grey-level of a pixel can be seen as its membership to the set of high-valued (bright) pixels. Some examples are shown in Figures 1 and 2. The objects presented in Figure 1 are generated by defining a membership function representing the area coverage of pixels by an ideal disk (square), positioned in the integer grid. For comparison, crisp counterparts are also presented. The fuzzy objects in Figure 2 are obtained by two different imaging techniques. To the left, an image of a hole in a piece of dark paper is obtained by an ordinary scanner set. The resulting circular object is very similar to the synthetic disk (Figure 1). Grey levels in the image reflect the area coverage of a pixel by the object, and can be naturally used as membership values (after scaling to $[0, 1]$). To the right, an MRA image of a cross-section of the aorta is presented; in this case grey-levels do not correspond equally well with the physical interpretation of the "membership of a pixel to the aorta", and a more advanced segmentation method may be preferable.

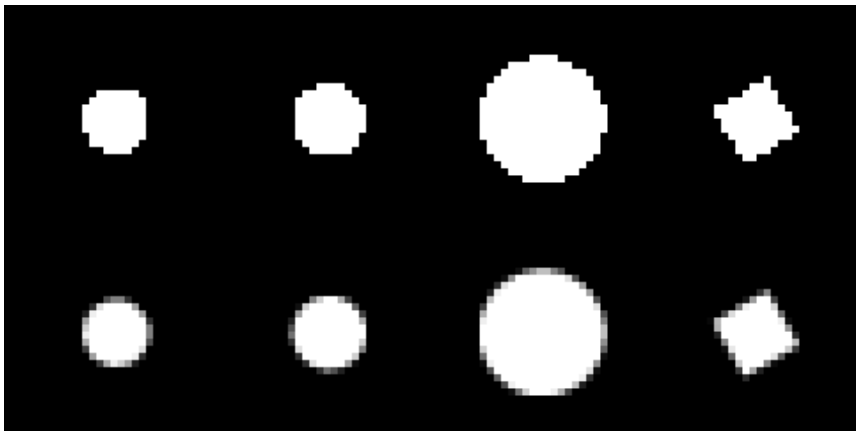

Figure 1: Examples of digitized objects with crisp (top) and fuzzy border (bottom)

One approach to get a more reliable information/representation is to integrate various features of the image into the fuzzy segmentation method. Another approach, based on the different interpretation of membership grades in a fuzzy region, is to retrieve information about the contour imprecision by comparing and merging several crisp representations of a region. The memberships are obtained by pooling the shapes derived from parallel application of several classical segmentation methods.

1.4 First and second twenty years

Almost forty years ago (1965), fuzzy sets were introduced by Zadeh, [50]. Twentyfive years ago (1979), Rosenfeld introduced fuzzy sets into image analysis [33]. The results obtained in the first five year period (1979-1984), are reported in [35]; various definitions, methods for measuring geometrical and other properties and relationships related to the regions in an image defined as fuzzy sets are summarized.

Today, the concepts suggested in [35] are still used as guide-lines in research on fuzzy image subsets, their geometry, and basic properties.

The fuzzy shape analysis techniques addressed in [35] are:

- Connectedness and surroundedness;
- Adjacency;
- Convexity and starshapedness;
- Area, perimeter, and compactness;

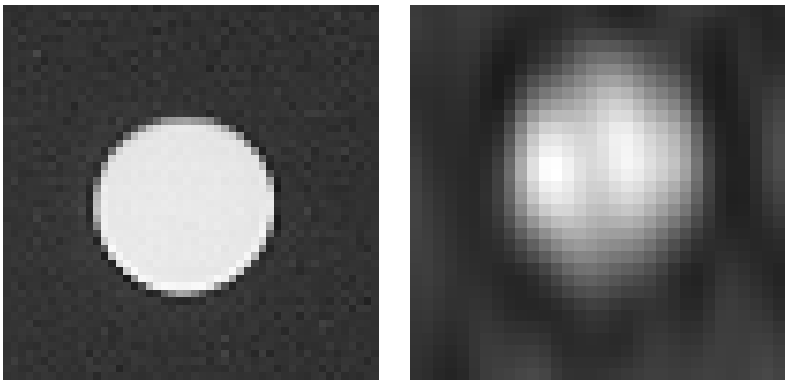

Figure 2: Left: A hole in a piece of dark paper, obtained by a scanner. Right: MRA image of a cross-section of the aorta.

- Extent and diameter;
- Shrinking and expanding, medial axes, elongatedness, and thinning;
- Grey-level-dependent properties; splitting and merging.

The results related to the first two topics are already exploited, and further developed in various fuzzy segmentation techniques; the topology of fuzzy image subsets still provides many challenges to deal with, and the first two items from the list above will certainly be further considered in that work.

Being interested in properties of fuzzy shape, we focus on the remaining topics from the list, as well as others related to shape analysis, developed later, and not mentioned above. However, the fact that [35] is, during the last twenty years, still one of the main references in most of the papers dealing with fuzzy shapes, indicates not only its outstanding significance and quality, but also the lack of research and results in the field since then.

2 Shape definitions

In [14], basic fuzzy geometric shapes, like point, line, circle, ellipse, and polygon, are defined on continuous 2D support space. The definitions are based on the α-cuts (in [14] called level sets) of a fuzzy set. It is assumed that the fuzzy set, given as a mapping $\mu : R^2 \to [0, 1]$, has a bounded support, is piecewise constant, and has a finite number n of distinct membership values.

Definition 1 *A fuzzy point is a fuzzy set with nonzero membership only at one point of the support space.*

Definition 2 *A fuzzy straight (curved) line is a fuzzy set for which any α-cut, $\alpha \in (0, 1]$, is either empty, or a straight (curved) line in a support space.*

A fuzzy line is a connected fuzzy set. A fuzzy straight line is a convex fuzzy set. Two fuzzy lines intersect at a fuzzy point if, for a non-zero value of α, their α-cuts intersect at a point.

Translation, rotation and dilation of a fuzzy set are defined. These transformations generate equivalent classes of fuzzy shapes. By using these transformations, a fuzzy line parallel, and perpendicular, to a given fuzzy line are defined; the first one is defined as a line obtained from a given one by translation, while the other one is a result of a translation and rotation of 90°.

In a similar manner, some basic fuzzy shapes are defined.

Definition 3 *A fuzzy circle is a fuzzy set whose α-cuts, for $\alpha \in (0, 1]$, are all concentric circles.*

Consider the definition of a fuzzy disk given in [35], where a membership of a point to a fuzzy disk depends only on the distance of the point to the centre of the disk. A fuzzy circle, according to 3, is a special case of a fuzzy disk, i.e., a fuzzy circle is a fuzzy convex fuzzy disk. It should be noted, however, that the terminology used in 3, does not correspond to the well accepted one for the crisp case, where a circle is a boundary of a disk.

Definition 4 *A fuzzy ellipse is a fuzzy set whose α-cuts, for $\alpha \in (0, 1]$, are ellipses with the same center, orientation, and eccentricity.*

In a similar way, by using α-cuts, a fuzzy polygon is defined.

For the fuzzy geometric objects, the membership is non-increasing away from the interior of the object. It seems natural to define complementary shapes by the membership which is non-decreasing away from the interior. In such way, fuzzy circular hole, fuzzy elliptic, and polygonal hole, are defined. A complementary α-cut is defined as

$$\mu_\alpha = \{p \in R^2 \mid \mu(p) \leq \alpha\},$$

and the definitions of fuzzy shapes can be adjusted to use complementary α-cuts and define complementary shapes, i.e., holes.

Examples of a discrete fuzzy disk, ellipse, and rectangle, as well as a fuzzy disk with a circular fuzzy hole, are presented in Figure 3. The area coverage principle is used to define the membership of a pixel to a shape. It should be noted, however, that the obtained discrete objects are not discrete fuzzy shapes in the sense of shape definitions given in this Section. The area coverage fuzzification principle does not guarantee that every α-cut of a discrete object is an object of the same shape, even though the principle is based on discretization of such (α-cuts of a) continuous fuzzy shape. It is obvious that discretization

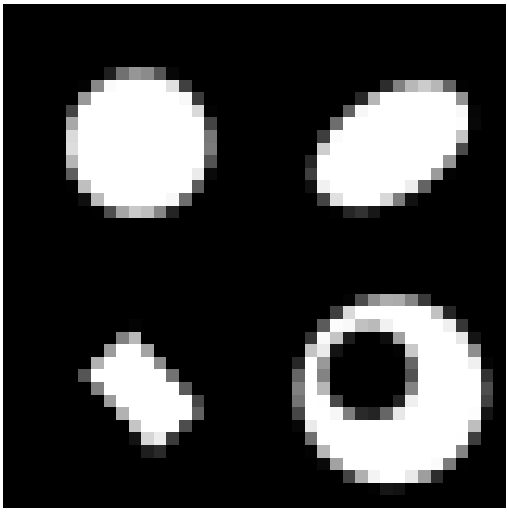

Figure 3: Examples of discrete fuzzy shapes.

affects significantly the properties of the (fuzzy) continuous objects. The transition from continuous to discrete fuzzy shape analysis is often not straightforward.

Definitions of a fuzzy point and a fuzzy line are studied in [11], as well. Those suggested there are more general. A fuzzy point (a, b) is defined by a membership function which has a value 1 for the real point (a, b), and all the α-cuts which are compact, convex subsets of R^2. Various definitions of a fuzzy line are given; they are mostly based on incorporating fuzzy numbers in the different forms of the standard equation of a crisp straight line.

The results are further studied in [49], where a general approach for deriving fuzzy concepts in plane geometry is presented.

3 Scalar descriptors

3.1 Definitions

The definitions listed below are given by Rosenfeld, [34] and [36]. All of them refer to fuzzy shapes with a continuous support.

The *area* of a fuzzy set $S \subseteq X$, given by its membership function μ_S, is defined as

$$A(\mu_S) = \int_X \mu_S(x)\, dx,$$

which is a generalization of the definition of the area of a crisp set.

The *perimeter* of a fuzzy set S given by a piecewise constant membership function

(also called fuzzy step set) μ_S, is defined as

$$P(\mu_S) = \sum_{\substack{i,j,k \\ i<j}} |\mu_{S_i} - \mu_{S_j}| \cdot |A_{ijk}|,$$

where A_{ijk} is the k^{th} arc along which bounded regions S_i and S_j, defined by (constant-valued) membership functions μ_{S_i} and μ_{S_j}, meet. This definition is a generalization of the perimeter of a crisp set. For a more general case, where a fuzzy set is given by a smooth membership function, its perimeter is obtained by an integration of the magnitude of the gradient of the membership function.

The *height* of a set S, given by μ_S, is defined as the integral of its projection on a vertical line:

$$h(\mu_S) = \int \max_x \mu_S(x, y)\ dy,$$

and similarly, the *width* of S is

$$w(\mu_S) = \int \max_y \mu_S(x, y)\ dx.$$

The *extrinsic diameter* of μ_S is defined as the supremum of the integrals of its projections:

$$e(\mu_S) = \max_u \int \left[\max_v \mu_S(u, v)\right] du,$$

where u and v are any pair of orthogonal directions.

For a connected fuzzy set (note: a fuzzy set is connected iff all its α-cuts are connected), the *intrinsic diameter* is defined as

$$i(\mu_S) = \max_{P,Q} \left[\min_{\varrho_{PQ}} \int_{\varrho_{PQ}} \mu_S(u, v)\right],$$

where the maximum is taken over all pairs of points P, Q in the plane, and the minimum is taken over all paths ϱ_{PQ} between P and Q such that, for any point R on ϱ_{PQ} it holds

$$\mu(R) \geq \min[\mu(P), \mu(Q)].$$

Such paths always exist, since μ_S is connected. When the set is crisp, $i(\mu_S)$ reduces to the standard definition of intrinsic diameter (the greatest possible distance between two points in μ_S, where only paths lying in μ_S are allowed).

One way to define a *measure of compactness* of a fuzzy set μ_S is to calculate

$$\frac{P^2(\mu_S)}{4\pi A(\mu_S)}, \tag{4}$$

(or its inverse), which is the well-known P^2A-compactness measure.

3.2 Inter-relations

All the definitions listed above reduce to the corresponding customary definitions for crisp sets. However, some inter-relations which these notions satisfy in the crisp case, do not hold for the generalized (fuzzified) definitions, as given above.

For a crisp (continuous) set S, the inequality

$$A(\mu_S) \leq h(\mu_S) \cdot w(\mu_S)$$

holds. However, for a fuzzy set, with area, height and width defined as in Section 3.1, it holds that

$$A(\mu_S^2) \leq h(\mu_S) \cdot w(\mu_S),$$

and μ_S^2 in this inequality cannot be replaced by μ_S. Even though for a crisp set $\mu_S^2 = \mu_S$, and the above definitions provide, formally, the analogy with the result holding for a crisp case, the difference is essential.

Moreover, if the set is crisp and connected,

$$e(\mu_S) \leq i(\mu_S); \tag{5}$$

if the set is crisp and convex, the equality holds. In the fuzzy case, however, it is possible to have $e(\mu_S) > i(\mu_S)$, even for a convex fuzzy disk. As an example, take a fuzzy disk D, with a membership function

$$\mu_D(x,y) = \begin{cases} 1, & x^2+y^2 \leq 0.5^2 \\ 0.5, & 0.5^2 < x^2+y^2 < 1.5^2 \\ 0, & \text{otherwise} \end{cases} .$$

For this set

$$e(\mu_D) = 1 \cdot 0.5 + 1 \cdot 1 + 1 \cdot 0.5 = 2,$$

while

$$i(\mu_D) = 1 \cdot 0.5 + 0.5 \times 0.5 \cdot \pi + 1 \cdot 0.5 = 1 + \frac{\pi}{4} < 2.$$

For a crisp set, it holds that $i(\mu_S) \leq \frac{1}{2}\ p(\mu_S)$. In [34] it is shown that the same inequality holds for a fuzzy set only if it is convex.

Based on the isoperimetric inequality,

$$4\pi A(\mu) \leq P^2(\mu), \tag{6}$$

the P^2A measure (4) is lowest for the crisp disc, compared to any other crisp set. In other words, the P^2A measure is the lowest for the most compact shape, and in that case is equal to 1. However, for fuzzy sets and definitions given in Section 3.1, the isoperimetric inequality does not hold in general. Moreover, for fuzzy disks, defined in a way that the membership function decreases (only) with respect to the distance from some point, taken

as an origin, the inverse inequality takes place. It can be shown that the compactness measure (4) decreases, i.e., that the compactness increases with the increase of fuzziness. This result is rather unintuitive.

In [8] the definitions given in Section 3.1 are modified in a way that they still reduce to their customary crisp counterparts, but the the relations (5) and (6) are fulfilled for a wide class of fuzzy (continuous) sets.

The idea followed in [8] was to make the inequality $A(\mu^2) \leq h(\mu) \cdot w(\mu)$ hold in a "proper" way, (i.e., $(A(\mu) \leq h(\mu) \cdot w(\mu))$, and let the changes needed to achieve that propagate to other definitions. For that purpose, $\sqrt{\mu}$, instead of μ, is considered in the definition of a projection, which introduces the same change in the definitions of height, and width, as well as diameter and perimeter of a fuzzy set. In that way, the isoperimetric inequality holds for continuous fuzzy sets, as well.

Area, perimeter and compactness measure of a discrete fuzzy set are studied in [41], where discrete fuzzy shapes are defined by a membership function based on the area coverage of a pixel (see Figure 3). The transition from continuous to discrete fuzzy shapes is obtained by interpreting a membership function of a discrete fuzzy set as a piece-wise constant continuous function (so-called step-function). However, discretization introduces additional inconsistency with the properties of crisp continuous sets. For example, the compactness measure, derived from the iso-perimetric inequality, for a discrete crisp disk is not in general equal to 1 and , even more, 1 is not the extreme value of the compactness measure, as it is in the continuous case. This property, as a consequence of discretization, propagates to the case of fuzzy discrete sets.

The focus of the research presented in [41] is on the precision of the estimation of the perimeter and compactness measure, when a discretized shape is used. A statistical study of discrete fuzzy disks having radii up to 20 pixels shows that the precision of the area and perimeter estimation increases when introducing fuzziness, and that the improvement (compared to the crisp case) is more significant for small objects (low resolutions). It is also shown that the compactness measure, incorporating perimeter defined as in Section 3.1, of the discrete fuzzy shapes has a similar behaviour. For all these measures, area, perimeter and compactness, it holds that increased fuzziness leads to increased accuracy. As a consequence, a crisp discrete disk is less compact than a fuzzy discrete disk, whose compactness measure is a more accurate approximation of the real disk. This property of a compactness measure is useful for estimations, but it is not intuitive.

The definitions suggested in [8], when adjusted to discrete shapes, lead to that the compactness measure (4) indicates the crisp discrete disk as the most compact fuzzy discrete shape. The consequences of introducing these definitions propagate to the compactness measure not only by giving a value higher than one, but also to give it a more intuitive behaviour. However, the measure gives high over-estimates, and therefore it is less appropriate for approximations of real shape compactness measure. Statistical results are shown in Figure 4. The different curves denote different levels of fuzziness.

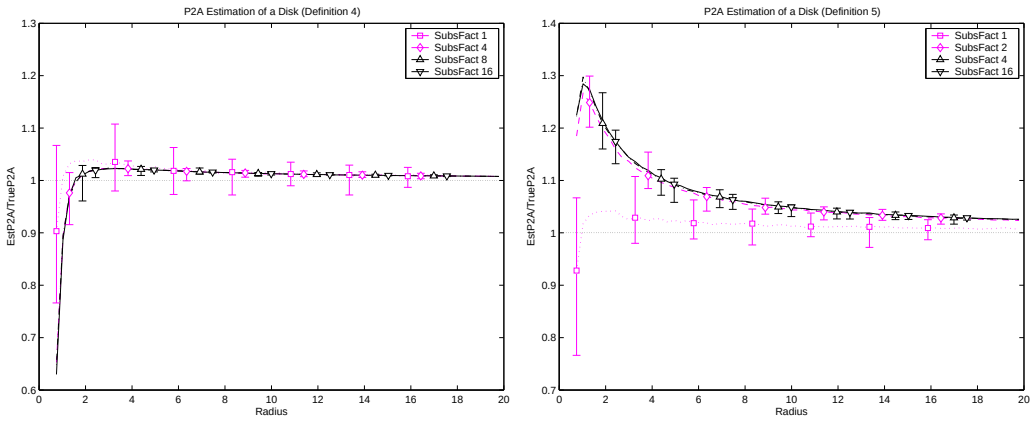

Figure 4: P^2A measure estimation for digitized disks. Left: Results based on definitions in Section 3.1. Right: Results based on modified definitions, [8] (from [41]).

3.3 General approach to the evaluation of parameters from fuzzy regions

If the imprecision included in the segmentation process can be captured using fuzzy regions, it seems natural and useful to carry over that imprecision to the parameters which describe the various features of the region. A general approach to the evaluation of parameters from fuzzy regions is studied in [16].

When R is a fuzzy region, with a membership function μ_R, it is seen as a nested uncertain region, under the form of a finite set $\{R_1 \subseteq R_2 \subseteq \ldots \subseteq R_n\}$ of regions, together with a basic probability assignment m defined from μ_R by

$$m(R_i) = \alpha_i - \alpha_{i+1},$$

where $\alpha_1 = 1$, $\alpha_i = \mu_R(x)$ for any $x \in R_i \setminus R_{i-1}$ and $\alpha_{n+1} = 0$. Then

Definition 5 *The property f measured on a fuzzy region R yields a random number r, defined by the probability*

$$p_f(r) = \begin{cases} \sum\{m(R_i) \mid f(R_i) = r\} & \text{if} \quad r \notin \{f(R_i) \mid i = 1, \ldots n\}. \\ 0 & \text{if} \quad r \notin \{f(R_i) \mid i = 1, \ldots n\}. \end{cases}$$

The expected value $\underline{f}(R)$ of $f(R)$ is evaluated as

$$\underline{f}(R) = \sum_{i=1}^{n} m(R_i) \cdot f(R_i). \tag{7}$$

The expected value has already been proposed in the literature in order to measure some features of fuzzy sets. The area of a fuzzy region R,

$$A(R) = \sum_{x \in X} \mu_R(x)$$

defined for fuzzy regions as in Section 3.1, is equal to the expected area $\underline{A}(R)$, in the sense of (7). The same holds for the perimeter, and the height, of a fuzzy region; the definitions given in Section 3.1 are equivalent to their corresponding expected values, given by (7).

It is clear that any parameter which can be extracted from a region has a natural meaning for a fuzzy, or uncertain, region R, when defined by Definition 5, and (7). The center of gravity, the diameter, the orientation, the compactness, etc., can be defined this way. However, not all the definitions based on membership function are equivalent to the expected value (7). For example, for the extrinsic diameter $e(R)$ of a fuzzy region R, defined in [34], it holds

$$\underline{e}(R) \geq e(R),$$

where $\underline{e}(R)$ is the expected value of the extrinsic diameter.

3.4 Fuzzy feature values

The fuzzification principle may lead to a fuzzy, instead of a crisp number. Such a method is called *extension principle* [4], and assigns membership for a feature R, to have some particular value n, over a fuzzy set S, given by its membership function μ_S:

$$R(\mu_S)(n) = \sup_{R(S_\alpha)=n} \alpha.$$

Similar approach is considered in [16]. It is noted that the expected (crisp) value of the parameters of fuzzy regions may sometimes be insufficient, and fuzzy parameter values extracted from fuzzy regions may be desired, instead. Possible ways to achieve this, as presented in [16], are:

- The imprecision of $f(R)$ can be expressed by a fuzzy number $f(R)$ with a support equal to $[\inf_i f(R_i), \sup_i f(R_i)]$, and a modal value $\underline{f}(R)$.
- A more rigorous definition of the fuzzy interval, obtained by transforming the probability measure associated to $f(R)$ by Definition 5, into a possibility distribution $\pi = \mu_{F(R)}$ consistent with the probability measure.

4 Vector-valued descriptors

4.1 Fuzzy shape signature based on the distance from the centroid

In [12], a shape representation which combines boundary information and region information, in order to design a description of the shape that is truly invariant to translation within the digitization grid, is studied. A signature is a one-dimensional (1D) functional representation of a two-dimensional (2D) shape boundary. The simplest way to generate a signature is to traverse the boundary and plot the distance from the centroid to the boundary as a function of the angle, see Figure 5.

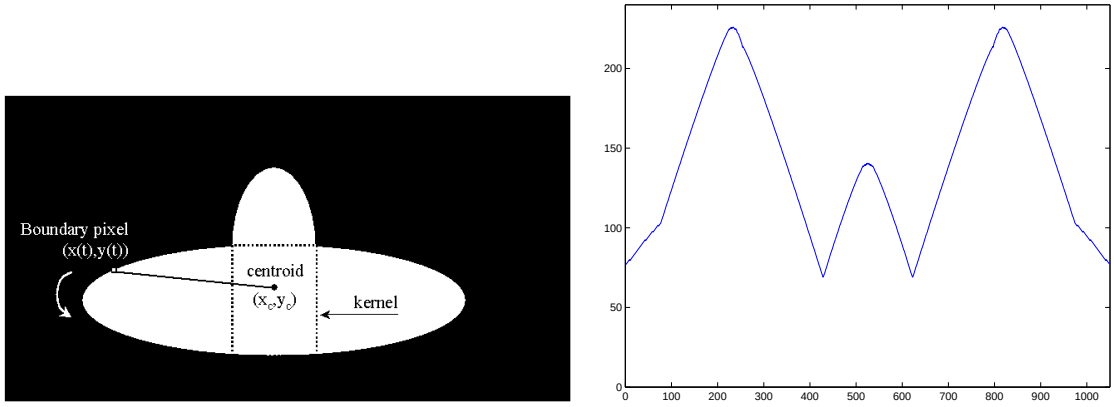

Figure 5: A star-shaped object and its corresponding shape signature (from [12]).

This shape signature function is extended to the case of discrete fuzzy star-shaped sets, having the centroid included in its kernel. Two methods are presented. The first method is based on the integration of a membership function over the considered straight paths, i.e., calculation of the length of a fuzzy line segment; the boundary of the fuzzy shape is considered to be the boundary of its support (the lowest α-cut), while the length estimation method is similar as the one presented in [37].

The second method processes each α-cut separately and averages the obtained signatures of binary shapes (based on the Euclidean distance), according to one of the fuzzification principles. In the continuous case, these two methods are equivalent for the class of star-shaped fuzzy objects having a centroid included in the kernel (for Definition of a star-shaped fuzzy object and a kernel of a fuzzy star-shaped object, see Section 5.1.1). However, the specific issues induced by the discretization lead to different performances of the proposed methods, when they are applied to discrete shapes.

The experiments show that the second method provides better results than the first one. The average SNR values obtained for 50 disks of each radius are presented in Figure 6, for increasing disk radius. It can be noticed that for both methods, the use of a fuzzy, instead of a crisp object, improves the description. However, for Method 1, the improvement tends to zero when the radius increases. Method 2 greatly outperforms Method 1, both in the crisp and in the fuzzy case. Furthermore, for Method 2 the advantage of using fuzzy objects is obvious and remains so also with the increase of the radius of the object.

The poor performance of Method 1 is not surprising, since the method relies on the discrete approximation of a straight line, and estimated length of a line segment, while Method 2 directly uses Euclidean distances. However, the first method can be seen as more general, since it can naturally be extended to shape signature calculation of non-star-shaped sets, while non-star-shapedness causes problems (in the crisp case, as well) when the second approach is used. The difficulties are related to the treatment of "exter-

nal" parts of the line connecting the centroid with the boundary point, where "external" becomes a rather subtle notion in relatively complex fuzzy topological issues. This is seen as a reason to be interested in a less efficient approach, as well.

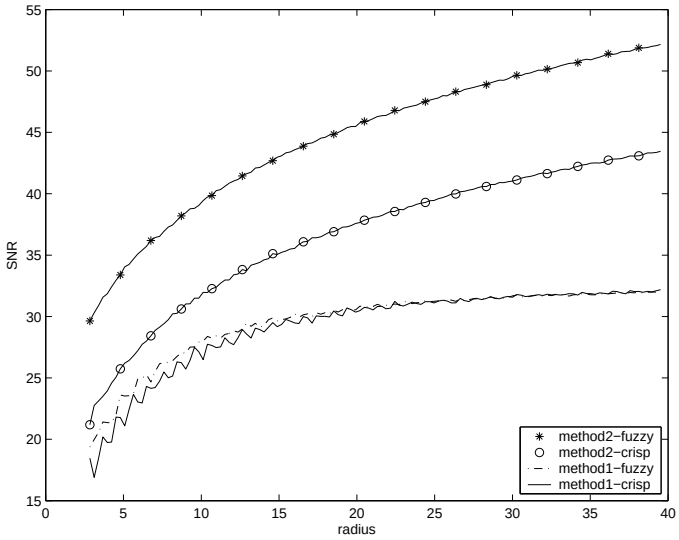

Figure 6: SNR of computed shape signatures for disks; comparative study of the two methods on crisp and fuzzy shapes (from [12]).

In any case, an important conclusion is that the use of fuzzy sets greatly improves the quality of the shape description; the sensitivity of the descriptor to the translation of the object within the digitization grid is highly reduced, compared to the crisp case.

4.2 Motion descriptors based on the Fourier transform

4.2.1 2D case

Shape descriptors based on the Fourier transform are both popular and efficient. They are often successfully applied to crisp shapes, where the main information about the shape is contained in the boundary of the object. Fourier descriptors are invariant under translations, rotations and change of the perimeter of the boundary. It is for sure useful to extend the concept to fuzzy shapes, but the first and very important difference is that a boundary of a fuzzy (grey-level) object is not well-defined. The method, if extended to fuzzy (grey-level) objects, should be applied to the whole object, rather than to only the boundary.

The approach presented in [17] relies on the idea of so-called motion descriptors, a family of invariants which remain unchanged under the motions of objects in 2D grey-level images. Using these invariants, similarity descriptors are defined. They are computed

by using the Fast Fourier Transform, and are stable, in the sense that if the difference between two objects is small, the difference between the invariants will also be small. This shape description method uses the whole fuzzy segmented image; no decisions about the (fuzzy) object boundary are made.

Starting with a Fourier transform $\bar{f} = \bar{f}(\psi)$ of a function f, and using polar coordinates (λ, ϑ) of a point ψ, a motion descriptor D_f^α of order α is defined as

$$D_f^\alpha(\lambda) = \int_0^{2\pi} |\bar{f}(\lambda, \vartheta)|^\alpha \, d\vartheta,$$

where $\bar{f}(\lambda, \vartheta)$ denotes the Fourier transform of f at a point (λ, ϑ). The motion descriptor $D_f^\alpha(\lambda)$ is invariant under translations, rotations, and reflections of objects. The invariance of a descriptor under the multiplication of f by a scalar can be obtained by normalization. The function

$$I_f^\alpha(\lambda) = \frac{1}{\|f\|_{L^1}^\alpha} D^\alpha f(\lambda)$$

is called the normalized motion descriptor of order α, of a function f.

Further, to achieve invariance under change of size of an object, the *similarity descriptor* of order α of f is defined:

$$J_f^\alpha(\lambda) = I_f^\alpha \left(\frac{\|f\|_{L^2}}{\|f\|_{L^1}} \, \lambda \right).$$

The similarity descriptor is a normalized motion descriptor with a particular sampling step, $\frac{\|f\|_{L^2}}{\|f\|_{L^1}} \, \lambda$, which provides invariance under change of size of an object, in addition to the invariance under translation, rotation, and reflection of objects.

It is proved that for two objects having the same shape, their similarity descriptors are the same. The main disadvantage of the similarity descriptor is that two objects can have equivalent descriptions, even if not being equivalent themselves (not obtained by a translation, a rotation or a reflexion from each other). Compensations for this disadvantage are that no previous knowledge is required about the type of a studied shape, the invariances are stable (they are similar for similar shapes), the computation is fast, and the interpretation of the result is very easy.

4.2.2 3D case

The shape descriptor described in [17] is further developed in [52] (although [17] does not exist in the list of references of [52]). A stable set of volume descriptors, invariant under the group of motions of the 3D Euclidean space, is derived for 3D grey-level objects, analogously as in the 2D-case. Due to the fact that the correspondence between the set of shapes and the set of their descriptors is not bijective, the similarity descriptors

cannot provide reconstruction of a shape. However, these descriptors are stable and, in addition, easy and fast to compute, different from, e.g., moment invariants, which provide recoverability, but need a lot of computational time when being of order larger than 3, and appear in rather complex expressions.

Examples of shape descriptions by the volume descriptor (VD) are presented in Figures 7 and 8. Equivalent shapes are described by (almost) the same VD function (Figure 7), while more or less different objects have different volume descriptor (Figure 8).

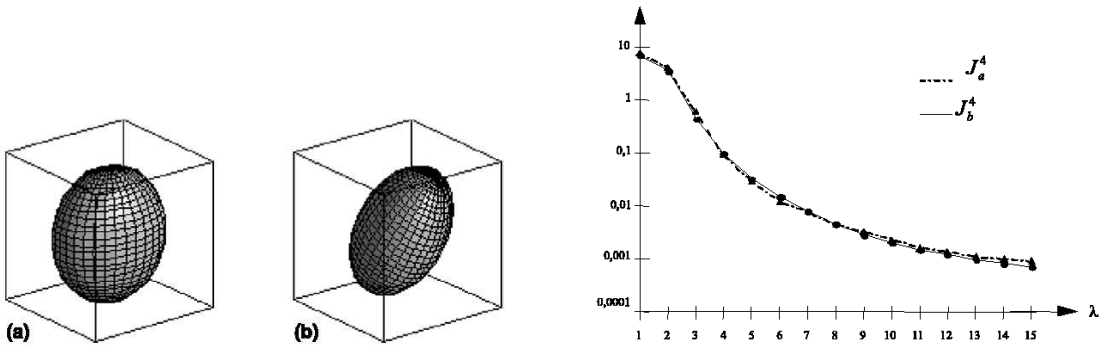

Figure 7: An ellipsoid (a) and a displaced ellipsoid (b). Volume Descriptors of objects (a) and (b) (from [52]).

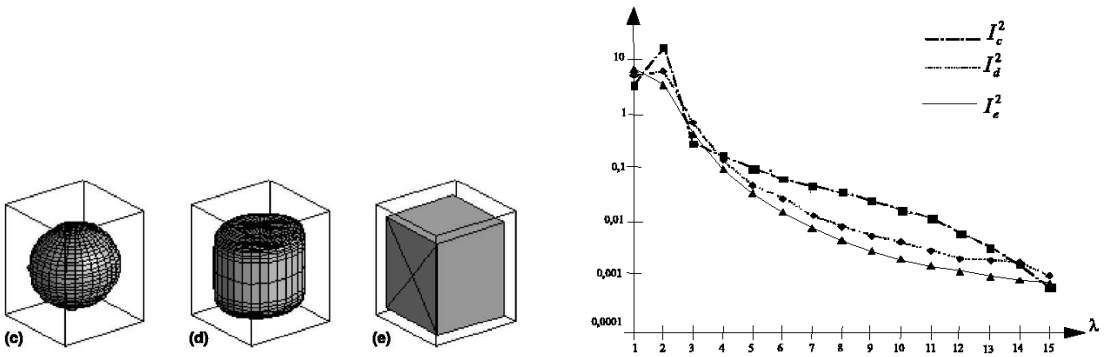

Figure 8: Three objects with different shapes. Volume Descriptors of objects (c), (d), and (e) (from [52]).

4.3 Description by moments

For a 2D continuous function $f(x, y)$, the moment of order $p + q$ is defined as

$$m_{pq} = \int_{-\infty}^{\infty}\int_{-\infty}^{\infty} x^p y^q f(x, y)dxdy \ ,$$

for $p, q = 0, 1, 2, \ldots$ In the case of discrete images, integration is replaced by summation over a bounded set. Moments are uniquely determined by the image, and moreover, they uniquely determine the image (if the set of moments is big enough). By using so-called normalized central moments, moment-invariants can be derived; they are invariant to translation, rotation and scale change, and thus are often used as shape descriptors.

Moments naturally "simultaneously" deal with both spatial and intensity properties of an image. The idea of incorporating fuzzy set theory into the shape description method based on moments is studied in [3]. However, this approach involves a more general definition of moments; essentially, the idea of summing the products of a spatial-related and intensity (membership)-related terms is what makes a connection, while the fact that distances, instead of spatial coordinates, are used introduces the difference to the classical notions.

The proposed descriptor provides a unique description of two alike but distinct images, and is invariant to rotation and size variation of the images. Being based on the fuzzy approach, the descriptor is less sensitive to noise and variation in illumination. It is successfully applied in inexact image matching.

The idea applied in [3] can be described as follows: a grey-level image is partitioned into non-overlapping blocks of equal size. Blocks contain regions of three possible types, "edge", "shade", and "mixed range" (additionally, edges are subdivided into different classes, depending on their slope). The degree of membership of a block to a certain class is defined by using some additional knowledge. Membership functions corresponding to the different classes are defined, by considering, e.g, average gradient, and variance. An "edge" is a contour of pixels within a block which has a large gradient with respect to its neighbours. A "shade" is a region with a small or no variation of grey-levels. A "mixed-range" is a region excluding edges and shades on a given image. Fuzzy reasoning is used to combine the information. The fuzzy moment, i.e., the membership-distance product of a block with respect to another block, is computed for all blocks obtained in the partition. A feature called "sum of moments", which keeps track of the image types and their relative distances, is used as image descriptor. The set of sums of fuzzy moments is stored in a one-dimensional array in a descending order, for each observed feature.

The number of blocks affects both time complexity and success of the description. It is noted that for a 512×512 pixel image the block size should be approximately 32×32 pixels to have a good matching result.

Normalization of a Euclidean distance between each two blocks of an image with respect to the image size itself provides insensitivity of a description to size variation. Rotation invariance is achieved by sorting the description vectors to keep the blocks with the most predominant features at the beginning of the array.

Incorporation of fuzzy membership functions and non-linearity of mappings reduce the effect of noise on the whole process.

5 Shape representation (non-numerical descriptors)

5.1 Convexity

5.1.1 Definitions

Definition 6 *A fuzzy subset S of a reference set X, given by its membership function $\mu_S : X \to [0,1]$, is convex if for all $P, Q \in X$ and all R on the line segment $\overline{PQ}$ it holds*

$$\mu_S(R) \geq \min\{\mu_S(P), \mu_S(Q)\}.$$

If S is crisp, the definition reduces to the standard one.

An equivalent definition of a convexity is that a fuzzy set is convex if and only if all its α-cuts, for $\alpha \in [0,1]$, are convex.

If a cross-section of a fuzzy set S with a line l is defined as a restriction of μ_S to l, then it holds that S is convex if and only if all its cross-sections are convex.

The convexity property has been exploited in many applications of fuzzy sets; convexity is central to some metric definitions and to some topological properties of the corresponding metric spaces of fuzzy convex sets. It can be used for formulation of decomposition criteria, in the shape description procedures.

Definition 7 *A crisp set K is star-shaped from a point $P \in K$, if for each point $Q \in K$, the line segment $\overline{PQ}$, joining P to Q, is contained in K.*

Definition 8 *A fuzzy set is star-shaped from P if and only if its α-cuts are all star-shaped from P.*

A fuzzy set S is star-shaped from a point P if its cross-sections through P are all convex. Obviously, a fuzzy set S is convex if it is star-shaped from each of its points. Fuzzy star-shaped sets, and many of their properties, reduce to the well-known properties of crisp star-shaped sets.

The kernel $kerK$ of a star-shaped set K is defined as a set of all points $P \in K$ such that the line segment $\overline{PQ}$ is contained in K, for each $Q \in K$. In other words, kernel contains all the points with respect to which the set is star-shaped. The fuzzy kernel of a fuzzy set is defined in [15]:

Definition 9 *Let $ker(S)$ be the set of Q such that S is fuzzy star-shaped with respect to P. For a fuzzy star-shaped set, fuzzy kernel $fker(S)$ is defined by*

$$[fker(S)]_\alpha = ker[S]_\alpha,$$

for $\alpha \in [0,1]$.

The intersection and the union of two fuzzy star-shaped sets, S_1 and S_2, such that $ker(S_1) \cap ker(S_2)$ is non-empty, is star-shaped. This proposition is not true for the (fuzzy) union of (fuzzy) convex sets, so fuzzy star-shaped sets extend fuzzy convexity in an important way, while, as shown in [15], many topological properties of spaces of fuzzy star-shaped sets remain similar to their fuzzy convex counterparts.

The convex fuzzy hull, $conv(A)$, of a fuzzy set A is defined as the smallest convex fuzzy set containing A.

The convex deficiency of S is the area of

$$conv(\mu_S) - \mu_S,$$

where $(\mu_A - \mu_B)(P) = \min\{\mu_A(P) - \mu_B(P), 0\}$, and the area of a fuzzy set is defined by integration. Normalized convex deficiency (e.g., by the area of a convex hull of a set), can be seen as a measure of the degree of concavity of a set S.

A complementary shape of a convex fuzzy set is a concave fuzzy set. Formally, such set is defined by

Definition 10 *A fuzzy set S of a reference set X is a concave fuzzy set if for all $P, Q \in X$ and all R on the line segment $\overline{PQ}$ it holds*

$$\mu_S(R) \leq \max\{\mu_S(P), \mu_S(Q)\}.$$

5.1.2 Fuzzy convex hull

A method of computing the convex hull of a fuzzy subset is presented in [13]. It is assumed that the fuzzy set has a bounded support and a finite number of distinct membership values in $[0, 1]$. The fuzzy shapes in discrete images fulfill these assumptions.

To determine the fuzzy convex hull of a fuzzy set, the convex hull of each α-cut is determined, and the fuzzification principle is aplied to the stack of crisp (convex) α-cuts.

Another approach for computation of a discrete convex hull of 2D grey-level images is presented in [26]. The presented method is purely discrete, and based on simple local computations. The resulting convex hull approximation fulfills convexity both in terms of geometric and grey-level information. In order to take grey-level information into account, but still use the methods developed for binary images, a 2D grey-level image is transformed into a 3D binary image, in a way that for each point its grey-level value becomes its third co-ordinate. The correspondence between grey-level g and z value depends on the application. An example of the original grey-level (a) and corresponding 3D representations (b) are shown in Figure 9. The inverse conversion is straight-forward. A method for computation of a convex hull of an object in 3D binary image is then applied. Covering polyhedra of the volume objects are created by filling local concavities. Local concavities are defined by the number and the configuration of neighbouring object voxels. The resulting covering polyhedron is convex and includes the convex hull. The difference

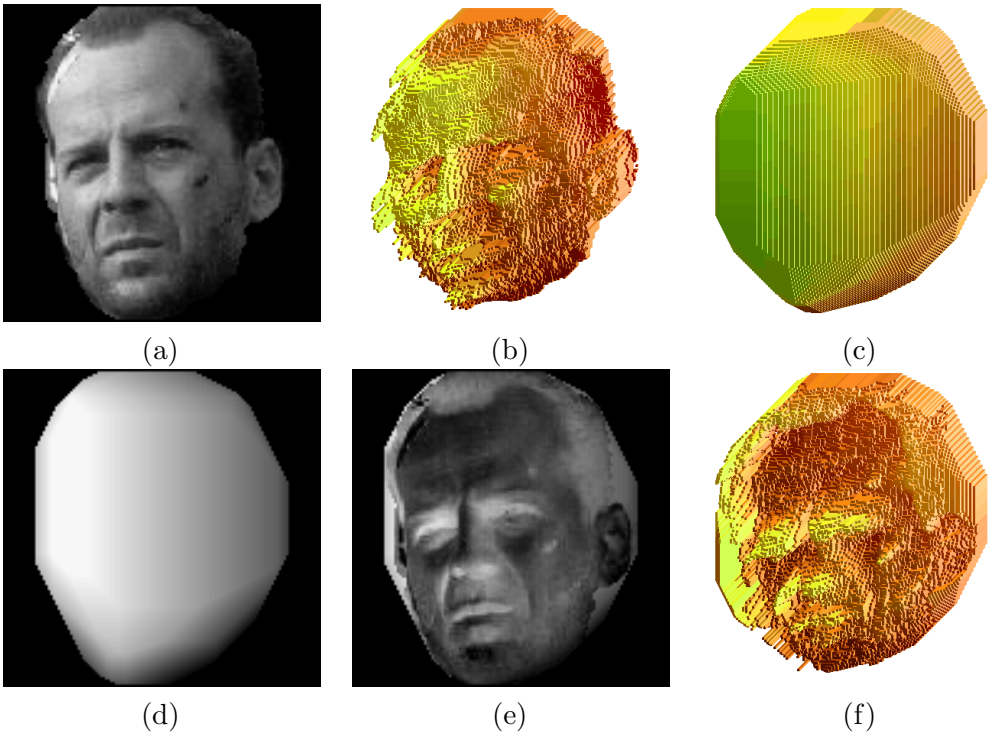

Figure 9: Grey-level convex hull computation and analysis. (a) A photograph of a face. (b) The 3D representation of the face. (c) The convex hull of (b). (d) The grey-level representation of (c). (e) The grey-level concavity regions, i.e., the difference between (d) and (a). (f) The 3D representation of (e) (from [26]).

between the covering polyhedron and the convex hull is reasonably small. The resulting 3D convex hull is projected back to a 2D grey-level image g, i.e., the grey-level convex hull.

The performance of the method is shown on the set of images in Figure 9.

5.1.3 Convexity indicators

A fuzzy set theory can be incorporated in the design of convexity indicators for (both binary and) grey-level (fuzzy) images. As presented in [32], convexity indicators measure the degree of convexity of an object in an image, using fuzzy inclusion indicators. Inclusion indicator $I(A, B)$ gives the degree to which a fuzzy set is a subset of another fuzzy set [39]. An inclusion indicator is defined as a two-argument function, mapping two fuzzy sets, A and B, to the interval $[0, 1]$ and satisfying nine particular properties (axioms):

A1 $I(A, B) = 1 \Leftrightarrow A \subset B$;

A2 $I(A,B) = 0 \Leftrightarrow \{x|\mu_A(x) = 1\} \cap \{x|\mu_B(x) = 0\} \neq \emptyset$.

A3 $B \subset C \Rightarrow I(A,B) \leq I(A,C)$.

A4 $A \subset C \Rightarrow I(A,B) \geq I(C,B)$.

A5 $I(A,B) = I(A+t, B+t)$, for any translation t.

A6 $I(A,B) = I(B^C, A^C)$.

A7 $I(A \cup C, B) = \min[I(A,B), I(C,B)]$.

A8 $I(A, B \cap C) = \min[I(A,B), I(A,C)]$.

A9 $I(A, B \cup C) \geq \max[I(A,B), I(A,C)]$.

The union and intersection of two fuzzy sets is computed as the pointwise maximum and minimum, respectively, of their membership functions, while $A \subset B$ means $\mu_A(x) \leq \mu_B(x)$ for every x in the reference set. Note that the axioms are not independent.

Inclusion indicators can be defined by using (different) fuzzified union and complementation:

$$I(A,B) = \inf_{x \in S}(A^C \cup B)(x).$$

The other approach is to use the fuzzification principle based on α-cuts, and define

$$I(A,B) = \int_0^1 \inf_{x \in A_\alpha} \mu_B(x) d\alpha.$$

However, this inclusion indicator fulfils the axioms A7 and A8 only as inequalities.

For a given indicator and a fuzzy set, fuzzy erosion and fuzzy dilation operations are defined.

Starting from a property of a crisp compact set X, that it is convex if and only if $2X = X \bigoplus X$, where $\bigoplus$ is a Minkowski addition and λX denotes homothety, a convexity indicator of the fuzzy set A with respect to the inclusion indicators I_1 and I_2, is defined as

$$c[I_1, I_2](A) = I_1(\delta_A(A), 2A).$$

A homothety λX for $\lambda > 0$, is defined by

$$\mu_{\lambda X}(x) = \begin{cases} \mu_X\left(\frac{1}{\lambda}x\right) & \lambda \neq 0, \\ 0 & \lambda = 0, x \neq 0, \\ 1 & \lambda = 0, x = 0. \end{cases}$$

The dilation δ is defined as an operation dual to the erosion,

$$\delta_A(B) = (\varepsilon_{-A}(B^C))^C$$

where the erosion is

$$\mu_{\varepsilon_A(B)}(x) = I_2(\tau_x(A), B),$$

and the translate of a set X by a vector a is a set $\tau_a(X)$ given by

$$\mu_{\tau_a(X)}(y) = \mu_X(y - a).$$

Different inclusion indicators, and consequently, different convexity indicators, are studied and analyzed. The choice of the indicator may be done with respect to the specific application.

Note: Basic morphological concepts for fuzzy sets are presented in more details in Section 5.4.

5.2 Symmetry

Symmetries are good candidates for describing shape. It is a powerful concept that facilitates object detection and recognition in many situations. Symmetry may be defined in terms of three linear transformations in n-dimensional Euclidean space: reflection, rotation, and translation. A set S is symmetric with respect to a linear transformation T if $T(S) = S$. In [42] a reflection symmetry is analyzed, and a procedure for detection of a reflection line is presented. Opposite from most of other methods for symmetry detection, based on edge or contour or set of point information, the one presented in [42] uses gradient information from a grey-scale image (so, no segmentation is needed), by analyzing the shape of the orientation histogram. The method should be equally applicable to fuzzy objects.

The idea is to determine the orientation of the gradient vector in each object surface point, where the object surface is defined by the grey-level function. The histogram of the gradient orientation, ranging from 0 to 360 degrees, can be obtained. The orientation histogram of a symmetrical object is symmetrical, and also periodic with period 2π, see Figure 5.2.

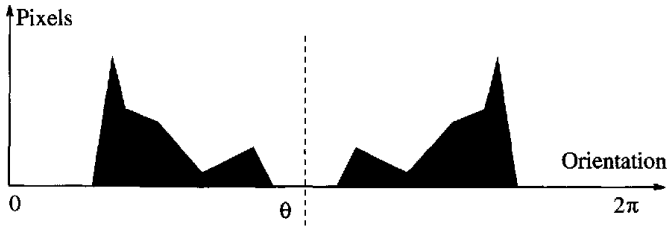

Figure 10: Typical shape of the gradient orientation histogram for a reflection symmetry object (from [42]).

The function

$$c(x) = \sum_{\theta=0}^{\pi} h(x+\theta)h(x-\theta)$$

calculated for each orientation x in the histogram h will reach its maximum for the symmetry axis orientation. The function $c(x)$ is a symmetry measure. It can be used to detect more than one symmetry axis, in which case it has more than one peak.

The position of a symmetry line (after its orientation is obtained) can be determined by, e.g., using a center of gravity, or projecting the original image onto a line perpendicular to the symmetry axis, and analyzing the profile of the projection.

The gradient image is obtained by using the Sobel operator. The obtained histogram is circularly smoothed, i.e, the angular data should be circularly continuous.

5.3 Distances and distance transforms

As noted in [4], there are two main approaches in measuring distances considering fuzzy objects: the first one basically compares only the membership functions (values) representing the concerned fuzzy object(s), while the other one combines spatial distance between objects and membership functions. The second class of methods finds more general applications in image processing since these methods take into account both spatial information and information related to the imprecision attached to the image object(s).

The problems that can be addressed when fuzzy distances are concerned, are

- distances between two points in a fuzzy set;
- distances from a point to a fuzzy set;
- distances between two fuzzy sets.

All three types of distances can be applied in shape analysis. A typical application for the first type of distances consists of finding the best path in the geodesic sense in a spatial fuzzy set. Distances from a point to a set are used when computing distance from a point to a complement of a fuzzy set, i.e., performing distance transform. The distances between sets are used in shape matching.

Fuzzy distances are often defined by generalizing crisp distances. It should be mentioned that some of the definitions do not always satisfy the properties of a distance (or metric); more general proximity functions can be used, instead.

5.3.1 Bloch's fuzzy geodesic distance

In [5] a geodesic distance between points in a fuzzy set are studied. Geodesic distance is defined with respect to the reference set X; a geodesic distance $d_X(x, y)$ from x to y is the length of a shortest path from x to y, completely included in X. The definition

of a geodesic distance between two points of a fuzzy set which is shown to have the best properties relies on the degree of conectivity of two points. The degree of connectivity in a fuzzy set μ between x and y is defined by Rosenfeld ([35]) as

$$c_\mu(x,y) = \max_{L_i \in L} [\min_{t \in L_i} \mu(t)],$$

where L is the set of all paths between x and y. Let $L^*(x,y)$ denote the shortest path between x and y on which c_μ is reached; this path is not necessarily unique and can be interpreted as a geodesic path descending as little as possible in terms of membership degrees. Let $l(L^*(x,y))$ denote its length (the number of points along the path). Then the geodesic distance in μ_S between x and y is defined as

$$d_\mu(x,y) = \frac{l(L^*(x,y)}{c_\mu(x,y)}.$$

If $c_\mu(x,y) = 0$, then $d_\mu(x,y) = \infty$, which corresponds to the result obtained for the classical geodesic distance in the case where x and y belong to different connected components. The definition corresponds to the classical geodesic distance computed at the α-cut of μ at level $\alpha = c_\mu(x,y)$. In this α-cut x and y belong to the same connected component. The definition satisfies the following set of properties:

- the distance between any two points is non-negative;
- the distance between x and y is the same as the distance between y and x;
- the distance equals zero only between two spatially identical points;
- the distance is defined by the shortest path between x and y that "goes out" of μ "as little as possible", and tends to infinity if it is not possible to find a path between x and y without going through a point t such that $\mu(t) = 0$;
- the distance decreases when $\mu(x)$ and $\mu(y)$ increase;
- the distance decreases when $c_\mu(x,y)$ increases;
- the distance is equal to the classical geodesic distance if μ is crisp.

The triangular inequality is not satisfied, but from the given definition it is possible to derive a true distance, satisfying triangular inequality, while keeping all other properties:

$$d'_\mu(x,y) = \min_{t \in S} \left[\frac{l(L^*(x,t)}{c_\mu(x,t)} + \frac{l(L^*(t,y)}{c_\mu(t,y)} \right],$$

where S is the whole image space.

A step further can be to define a geodesic distance between two points in a fuzzy set to be not a crisp, but a fuzzy number, since for an imprecisely defined set the distances

within it may be also imprecisely defined. To achieve this, the extension principle based on a combination of the geodesic distances computed on each α-cut of μ can be used (see Section 3.4). If $d_{\mu_\alpha}(x, y)$ denotes the geodesic distance between x and y in the crisp set μ_α, the degree to which the geodesic distance between x and y in μ is equal to d is

$$d_\mu(x, y)(d) = \sup\{\alpha \in [0, 1], d_{\mu_\alpha}(x, y) = d\}.$$

Some properties of a fuzzy number defined in this way are, e.g., that the degree to which the geodesic distance between two points can be less than the Euclidean distance is zero and that the maximum of a fuzzy number representing the distance between two points is reached for the distance between them at the level (α-cut) of their connectedness.

5.3.2 Toivanen's distance transform on curved spaces

Two geodesic distance transforms for grey-scale images are presented in [44]. The first one, called the Distance Transform on Curved Space (DTOCS), performs the distance calculation with integer numbers. After the length of a path between two points is defined, a distance map in which the value of every pixel is the length of the shortest path to the nearest background pixel is generated. The DTOCS calculates the distance value for each point by calculating the grey-level difference between two adjacent point along the minimal path. The distance between two adjacent points is determined as an absolute value of a difference between their grey levels, increased by 1, which is used as an integer approximation of the length of a step on the grey level surface, using the chess board kernel for horizontal displacement estimation (see Figure 11). The parameter, related to the curvature of a grey-level image, is introduced to provide a possibility of different scaling of horizontal and vertical "components" of a displacement (horizontal step is 1, while the vertical can be e.g., $[0, 255]$, for 8-bit pixel size).

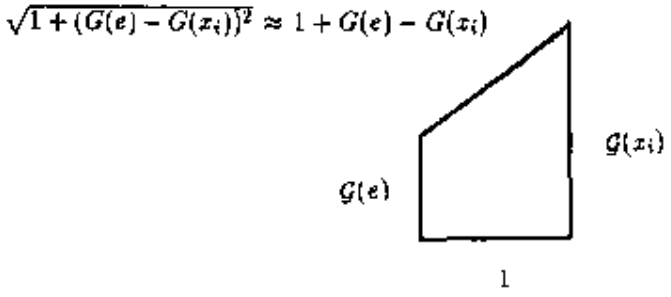

Figure 11: The height displacement of DTOCS for all 8-neighbours x_i of a pixel e, in a rectangular grid (from [44]).

The second presented distance transform is called the Weighted Distance Transform on Curved Space (WDTOCS) and gives a weighted distance map over a grey-level image. Each sub-distance along the path is Euclidean, i.e, the distances between two edge-neighbours is 1 and between two point neighbours is $\sqrt{2}$. Optimal propagating weights, 0.95509 for isothetic step, and 1.3693, for a diagonal step in a 3×3 mask, are used instead; this gives a better approximation of the (global) Euclidean distance. It is shown that both transforms converge to the correct distance map; depending on the size and complexity of an image, the number of iterations of two scans of an image needed is $3 - 10$.

In the so-called $\sqrt{2} - DTOCS$ distance transform presented in [18] step-lengths (horizontal displacements) 1 and $\sqrt{2}$ are used, instead of a chessboard mask, or optimal step-weights. This transformation is seen as a hybrid of chessboard and Euclidean distance definitions, but without as solid theorethical basis as for the DTOCS and the WDOTCS. The computation of both WDOTCS and $\sqrt{2} - DTOCS$ includes floating-point values calculations, which is computationally havier that working with integers. It is shown in [9] that using integer values 3 and 4 as weights for a horizontal and a diagonal step, respectively, gives better approximation of Euclidean distance than using the weights 1 and $\sqrt{2}$. It is left for a further investigation to find appropriate integer weights which would correspond to both horizontal and vertical displacement in grey-level images.

5.3.3 Borgefors and Svensson's distance transform for sets with fuzzy borders

A distance transform in images with fuzzy borders is proposed in [10]. The difference from a standard distance transform is in the initialization, which takes the fuzziness of the border into account. In the standard case, object pixels are initially set to infinity and background pixels to zero. In the fuzzy border weighted distance transform (fWDT) the initialization reflects the uncertainty of the border pixels. Except for the initialization step, the method uses standard chamfering technique.

In the digitization process, the pixels are assigned to the object, or to the background, according to some principle which usually creates jagged border of the digital object, due to the hard decision if the point belongs to the interior, or not. A whole interval of possible border positions between two points (one inside, and one outside) results in the same digital situation. In order to allow smoother transition between background and object to have an influence on the distance map, the initialization is done so that small distance labels are linearly distributed among pixels having grey-levels between two thresholds set to get "certainly inside" and "certainly outside" points. If, e.g., $\langle 5, 7 \rangle_{2D}$ distance transform is used (in the 3×3 neighbourhood), the smallest distance label assigned to the object point is 5; labels $1, 2, 3, 4$ are free to be used to initialize the fuzzy border, so that the position of a "real" border (between two extreme situations) does make a difference. It is important to use a distance transform for which the weight for a horizontal step is not too small, in order to get a more graded transition on the border, reflected by different initial values. Good choices in 2D are, e.g, $(6, 8)_{2D}$, $(8, 11)_{2D}$, $(9, 12)_{2D}$, $(10, 14)_{2D}$, for the 3×3

neighbourhood. After the initialization, the distance map is calculated in the standard way, i.e., by two raster scans over the image. In the distance map, points with labels smaller than half the length of a horizontal step are seen as most plausibly background, and those with labels larger than half of a horizontal step are most plausibly object points. The fWDT is not necessarily a metric, or even ordered in any way.

5.3.4 Saha's et al. distance transform for fuzzy sets

Another way of calculating distance transform for fuzzy sets (FDT) is proposed in [37]. The notion of fuzzy distance is formulated by first defining the length of a path on a fuzzy subset, and then finding the path with a minimal length, connecting two points. FDT is defined as a process on a fuzzy subset that assigns to a point its fuzzy distance from the complement of the support. It is shown that the fuzzy distance is a metric for the support of the object.

A path π between two points in a set S is a sequence of adjacent points of S, connecting these two points. The length of a path is equal to the number of points along the path. Only hard adjacency relations are considered to define a path. To define the strength of a path, the strength of a link pq (a path consisting of two points, p and q) is defined as, e.g.,

- $\max\{\mu(p), \mu(q)\} \times \|p - q\|$, or
- $\frac{1}{2}(\mu(p) + \mu(q)) \times \|p - q\|$.

In the continuous case, according to this approach, the length of a path between two points in the fuzzy set is obtained by integration of the membership function along the points forming the path between them. Adjusted to the discrete case, the integral is replaced by some discrete approximation (integration sum). In [37], the second definition of the strength of the link is used; it incorporates two components into the strength of a link – one coming from the membership values of p and q, and the other from the distance between these two points. The strength of a path is then defined as the sum of the strengths of the links along the path.

An algorithm for computing the FDT of digital objects is presented. The background (reference set) in the fuzzily segmented image is determined by thresholding. The spatial distances are determined for each point and its 8 neighbours, and the vector containing the distances is generated. For a crisp object, the shortest path from a point to the background is always a straight line, but for a fuzzy object that is not always the case. That is why the computation of FDT requires more than two scans of the image; the number of raster scans needed in the computation is dependent on the shape of the object. FDT is computed by using a dynamic programming-based approach.

Some examples of the application of FDT in medical imaging are presented, e.g., a computation of local thickness, a very useful parameter in analyzing object shape and

morphology, see Figure 12. It is noted that a skeleton generated from a fuzzy representation of an object would be a desirable starting point (since thickness is supposed to be computed along the skeleton of an object), but such skeletonization methods are not well developed yet. It is concluded that the FDT method promisses to be of significant value for structural object analysis, once the technique has been fully validated.

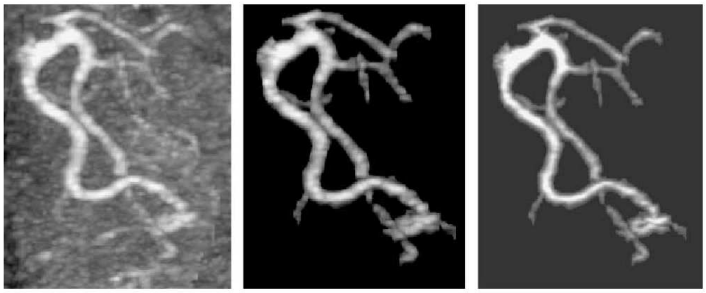

Figure 12: FDT-based thickness computation applied to an arterial tree. (a) A MIP rendering of a 3D subvolume taken from a 3D CTA image of a patient's head (after removing bones) showing a portion of the carotid arterial tree. (b) A MIP of the fuzzily segmented arterial tree. (c) A MIP of the FDT image of the 3D image shown in (b). Mean and standard deviation of the thickness values computed along the curve skeleton of the arterial tree mask are 2.7 and 1.8 mm, respectively (from [37]).

5.4 Fuzzy mathematical morphology

Mathematical morphology is a set-theoretic method for the extraction of shape information from a scene; it studies the transformations of an image when it interacts with a matching pattern (structuring element) through well-defined local operations. The basic ones are erosion, $E(A, B)$, and dilation, $D(A, B)$, defined by

$$\begin{aligned} E(A,B) &= \{y \in R^n \mid T_y(B) \subset A\} , \\ D(A,B) &= \{y \in R^n \mid T_y(B) \cap A \neq \emptyset\} . \end{aligned}$$

$T_y(B) = \{x \in R^n \mid x - y \in B\}$ is a translation of a set B by a vector y.

By varying the size and shape of the structuring element, it is possible to obtain useful geometrical and topological information of the different objects in the scene. Erosion reduces the image area, while dilation enlarges it, by reducing the background region. Opening (erosion followed by dilation) smoothes the contour from the inside, and suppresses small islands and capes; closing (dilation followed by erosion) smoothes the object from the outside by filling narrow bays. Due to these characteristics, an appropriate choice

of the structuring element together with a suitable combination of morphological operations can be successfully used for cleaning noise pixels, to compute the gradient of a scene, to detect the edges of the objects, to define the skeleton of the object [22], and to find simple shapes in the image.

Mathematical morphology cannot be directly extended to fuzzy sets, since it is not internal in the $[0,1]$ interval. In attempts to build a mathematical morphology which can process fuzzy sets, two major construction principles are followed [6]. One relies on the fuzzification principle, while the other is based on translating set equations into functional ones and involves the theoretical framework of triangular norms and conorms. The second construction principle leads to an infinity of definitions for the basic operators. In [6], various definitions for basic morphological operations are presented, analysed, and compared.

By following the fuzzification principle, see Section 1.2, fuzzy dilation and fuzzy erosion can be obtained from binary definitions. Depending on which of the equations (1) or (2) is used in the fuzzification process, fuzzified morphological operations are

$$\begin{aligned} D(\mu,\nu)(x) &= D_\nu(\mu)(x) = \int_0^1 \sup_{y\in(\nu_\alpha)_x} \mu(y)d\alpha, \\ E(\mu,\nu)(x) &= E_\nu(\mu)(x) = \int_0^1 \inf_{y\in(\nu_\alpha)_x} \mu(y)d\alpha, \end{aligned}$$

or

$$\begin{aligned} D(\mu,\nu)(x) &= D_\nu(\mu)(x) = \sup_{\alpha\in(0,1]} \left[\alpha \sup_{y\in(\nu_\alpha)_x} \mu(y)\right] \\ &= \sup_y [\nu(y-x)\cdot\mu(y)], \\ E(\mu,\nu)(x) &= E_\nu(\mu)(x) = \inf_y [\mu(y)\cdot\nu(y-x)+1-\nu(y-x)] \end{aligned}$$

The second approach is followed in [23], where several ways to design fuzzy morphology are studied and analysed. Some of them are based on the fuzzification of underlying logical operations, i.e., Boolean conjunction and Boolean implication, while others rely on fuzzifying set inclusion.

The most general approach of the first type is based on the generalization of negation, conjunction, and implication, see Section 1.2. Then, the fuzzy dilation $D_{\mathcal{C}}(A,B)$ and fuzzy erosion $E_{\mathcal{T}}(A,B)$ are defined by:

$$\begin{aligned} D_{\mathcal{C}}(A,B)(y) &= \sup_{x\in T_y(d_B)\cap d_A} \mathcal{C}(B(x-y),A(x)), \\ E_{\mathcal{T}}(A,B)(y) &= \inf_{x\in T_y(d_B)} \mathcal{T}(B(x-y),A(x)), \end{aligned}$$

where $d_F = \{x\in R^n \mid F(x)=t \text{ for some } t\in[0,1]\}$ is the domain of the function F.

The second group relies on an extension of a binary inclusion relation and assumes a mapping which assigns a number from a unit interval to a pair of fuzzy sets. Fuzzified set inclusion is then used to extend the binary erosion to operate on fuzzy sets. Fuzzy erosion is thus defined by using fuzzy inclusion I instead of the standard one, i.e., $E(A,B)(x) = I(x+B,A))$, while fuzzy dilation can be defined by duality with respect to the standard negator.

Different lists of desired properties of an inclusion indicator lead to different morphological operations.

In general, it is concluded that fuzzy morphological operations have weaker properties, compared to binary ones. For example, a condition $\nu(0) = 1$ is necessary and sufficient to guarantee the extensivity of dilation, and thus antiextensivity of erosion; it corresponds to the classical condition $0 \in B$. If this condition is not satisfied, it is possible to get more imprecision or uncertainty in an eroded fuzzy set than in the initial one (0 valued points in the initial fuzzy set may not be 0 valued in the eroded one). Second, a generalization of Matheron's representation [24, 38] cannot be derived for fuzzy morphological operations (it cannot be shown that any increasing spatially translation invariant operation can be represented by a union of fuzzy erosions). Third, fuzzy morphological opening and closing have weaker properties, and they are not morphological filters (increasing and idempotent mappings). Fourth, the property of binary mathematical morphology that it is not useful to apply the same operation twice is not valid. Well-defined properties of the operators (providing well controllable chaining of the operations) do not hold for fuzzy morphological definitions in general.

In spite of that, fuzzy mathematical morphology appears as a powerful theory as it provides a large set of operations that can be used in fuzzy image processing. It provides operations whose effects are spatially controlled; e.g., dilation allows us to propagate fuzziness to an extent defined by a structuring element. The applicability and importance of fuzzy mathematical morphology is also in the low sensitivity of fuzzy morphological operators to small changes of shapes; they provide degrees of fulfilment for the observed property, slightly different for slightly different shapes, which makes them useful in images slightly changed by noise.

In [22], an example of application of the basic morphological operations is shown. For a fuzzy image I and a structuring element SE of a size $s(SE)$, fuzzy erosion is defined as

$$\begin{aligned} E_{\min}(I,SE) &= \min\{1-|I-SE|\}, \quad \text{Minimum Erosion} \\ E_{\text{ave}}(I,SE) &= 1-\frac{1}{s(SE)}\sum|I-SE|, \quad \text{Average Erosion} \end{aligned}$$

while dilation is defined by using duality:

$$D(I,SE) = 1 - E(1-I,SE).$$

The use of different metrics in the definition of fuzzy operators is dependent on the particular problem; in an image with a high object connectivity, minimum erosion may be

sufficient to clean the image, while in a sparse image such operations may erase all relevant data if the size of the structuring element is not greater than the maximal connectivity between the pixels (in this case average erosion performs much better).

Minimum Erosion, with a flat 3×3 square as a structuring element, filters small background effects in the image, but also eliminates details that can be useful. Dilation enhances noise, background, and spurious effects, but when combined with erosion, it allows the retrieval of relevant geometric information. The opening of the image is cleaned and smoothed, and its components appear more separated. In closing, the image is smoothed too, but by filling the holes inside regions with higher intensities.

Another example of using fuzzy morphological operators in image processing is given in [6]. The application concerns data fusion in medical imaging. The aim is to combine several magnetic resonance images to improve the detection of spatial information. In these images, the imprecision is due both to fuzziness in contours in each image, and to imperfect registration between images. The first type of fuzziness is taken into account by representing edges in these images by a fuzzy set, depending on their strength. The second type is modeled by a fuzzy structuring element representing the the registration imprecision. The fuzzy dilated edge set then provides the location of the edges with graduations which represent both sources of imprecision. The fusion of such dilated fuzzy sets obtained from several images allows taking the decision using all the information about the problem and thus avoids the conflicts obtained from the fusions of crisp edges. The imprecision in spatial data is introduced and managed in a fusion and decision process, by means of fuzzy mathematical morphology.

5.5 Medial axis transform and skeletons

The Medial Axis Transform (MAT) [7] is a method which reduces an objects to its medial axis, or to its skeleton. If the pixels resulting from MAT are unmarked, the obtained image is binary and does not allow recovering of the original object; such shape representation is called *a medial axis*. If the resulting pixels are marked, a grey-level image is obtained, and the original object can be recovered from it; such shape representation is called *a skeleton*. It should be noted that the distinction between a medial axis and a skeleton is not always clear in the literature, and both names are used interchangably. In the following, we refer to the result of MAT as it is originaly done by the authors of the papers. The comments on the recoverability of the object from the described representations are given explicitely.

In [25], four equivalent definitions of the MAT of shapes in the real plane are given. The first one is the prairie fire model, where the MAT points are the locations where the propagating wavefront, initiated on the shape boundary, "intersects itself". This approach is illustrated in Figure 13(a). The second equivalent definition of MAT is based on the paths from a point to the boundary, i.e., on the distance from the point to the boundary (being the length of the shortest path between them). MAT is defined as the set of all points of S which do not belong to the minimal path of any other point, together with their distances. The skeleton is the planar projection of the ridges of the distance map

Figure 13(b). The third model considers the skeleton as the geometric location of centres of maximal disks. For a point P in a set S, the largest disk centered in P and fully contained in S is called maximal disk of S if it is not contained in any other disk, centered in any other point of S. The skeleton of a set S consists of the centres of its maximal disks, together with their radii. This approach is illustrated in Figure 13(c). The fourth model defines a MAT of a set as the set of points that do not belong to any straight line segment connecting other points to their respective closest boundary points, Figure 13(d).

These four definitions are not equivalent in the discrete plane. In order to apply them to the discrete plane, adjustments have to be made. Discrete versions of a straight lines, a path, a distance, and a disk have to be used.

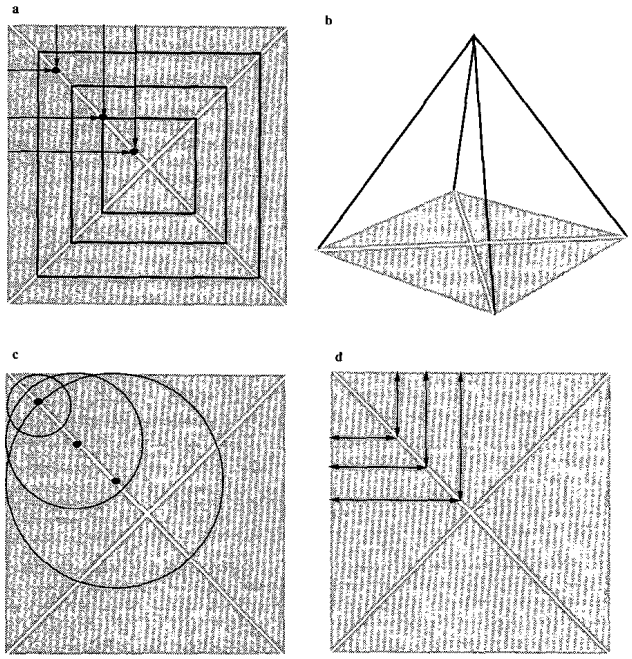

Figure 13: Illustration of four definitions of the skeleton (white) and an object (striped). (a) The black curves are offsets of the boundary obtained by constant velocity propagation. The set of self-intersecting points of the propagating curves is the skeleton. (b) The skeleton is the planar projection of the ridges of the distance map from the boundary. The ridges are shown as black curves in 3D, where the third dimension represents distance. (c) The skeleton is the set of centres of maximal disks. (d) The skeleton is considered as the set of points that do not belong to any straight line connecting other interior points to their respective closest boundary points (from [19]).

Several generalizations of MAT to the case of grey-value (fuzzy) images have been

proposed. Spatial Piecewise Approximation of neighbourhoods (SPAN) ([1]) is defined in terms of maximal homogeneous disks; the given image can be approximated started from the set of centres, radii, and average grey levels of the disks. The disadvantage of this approach is the computational cost of determining the maximal disks. Another generalization GREYMAT, or GMAT, [20], is based on the concept of grey-weighted distance: the grey-weighted length of a path is proportional to the sum (or integral) of the grey levels along the path, and the grey-weighted distance between two points is the lowest grey-weighted length of any path between them (compare to [37]). The GREYMAT of an image is defined as the set of points whose grey-weighted distance to the zero-valued background is a local maximum, together with their distances. The disadvantage of this approach is that it requires segmentation of an image into background and not-background. Still another generalization is GRADMAT [48], where a score is computed for each point P in the image, based on the gradient magnitudes at pairs of points that have P as their midpoint. These scores are high at the points that lie midway between antiparallel edges, or along angle bisectors, so they define a MAT-like (grey-valued) skeleton. However, this skeleton is very sensitive to noise and a subject of artifacts created by pairs of edges belonging to different objects.

A generalization of MAT to grey-level images, overcoming the disadvantages of the approaches presented in earlier works (SPAN [1], GREYMAT [20], and GRADMAT [48]), is presented in [31]. The approach is inexpensive to compute, does not require image to be segmented, and is unsensitive to noise. It is based on the fact that the MAT of a set S can be constructed by a process of iteratively shrinking and reexpanding S. For grey-scale images, the operations of local MIN and local MAX are generalizations of shrinking and expanding. The value in a point is replaced by the minimum, or maximum, of all values of the points within some given distance δ from the observed point. These definitions reduce to the ordinary shrinking and expanding, respectively, in the crisp case. If applied to a fuzzy image, they produce a fuzzy-valued output (values between 0 and 1). For the fuzzy set μ, $\mu_{-\delta}$ and μ_{δ} denote the results of shrinking, and expanding, of a set by performing MIN and MAX in a local neighbourhoud within distance δ. Such neighbourhood depends on the distance which is used; e.g., for $\delta = 1$ and the city block distance, it reduces to 4-neighbourhood, while for $\delta = 1$ and the chessboard distance it becomes 8-neighbourhood.

The medial axis of a fuzzy set μ is defined as

$$\sup_{\delta \geq 0} [\mu_{-\delta} - (\mu_{-\delta-1})_1)$$

where δ is an integer. In this way, medial axis is the set of pixels of all $\mu_{-\delta}$ that disappear when $\mu_{-\delta}$ is shrunk by one unit and do not appear when it is re-expanded by one unit.

The reconstruction of an image from its generalized (min-max) MAT is not possible (as opposite from the crisp case). If the whole sequence of changes produced during the medial axis detection is known for each point of the image, the reconstruction can be done, however requiring a large amount of information. This is a consequence of the fact that in the min-max medial axis construction process the value of each point may be changed

in every iteration, while in the crisp case it is changed at most once, from 1 to 0.

To assign the min-max MAT value to a point, e.g., the maximum, or the sum, of all the values (differences) obtained for the observed point during the process can be used.

Reconstruction of an image starting from min-max medial axis, and also from GRAD-MAT image, is studied in [47]. An exact reconstruction is possible, but needs a lot of information. However, a good approximate reconstruction can be obtained by using only those skeletal points which have high min-max MAT values, and only the few most significant components of their corresponding "difference" vectors. Some modifications of the min-max MAT, providing thin skeletons, are proposed.

In [30], an extension of Maximal Square Moving (MSM) algorithm, proposed in [46], to the grey-level and, in particular, fuzzy images, is given. The method is called the Weighted Maximal Square Moving (WMSM) algorithm; it operates on digitized pictures and produces a structure-descriptive representation of the core-line of an image, consisting of the centres of the maximal squares contained in the image, together with their size, average value of the membership values within it, and the coordinates of the centroids of the neighbouring squares. The points composing the core-line do not necessarily coincide with image pixels and are kept in a data structure from which syntactical or semantical representations of the original image can easily be obtained.

The algorithm is based on the definitions of runs and squares, and three operations on squares: enlarging, deriving, and meeting. By performing these operations and generating maximal squares contained in the image, while keeping track on the derivations and meetings made for each maximal square, information of the neighbouring maximal squares can be extracted. The center of a detected maximal square is computed as the center of gravity, where membership values of the points are used as weights.

In order to improve skeletonization results, and reduce the number of spurious branches, it is possible either to put some restrictions on the side length of the maximal squares, and disregard those which are too small, or to disregard squares having too low average membership value.

The fuzzy compactness measure proposed in [35] can be used for generating a skeleton of a fuzzy set, as well [27]. Optimal fuzzy thin skeleton is extracted by minimizing the compactness measure in the fuzzy skeleton plane in the image. From an optimal fuzzy skeleton thus produced, one may also obtain its crisp single pixel width version, by retaining only those pixels which have strong skeleton-membership value compared to their neighbours.

The skeleton extraction is done in three steps. The first step assumes fuzzy segmentation of the regions in the image. Various algorithms for minimizing ambiguity both in greyness and in spatial geometry are proposed in [28]. The algorithm extracts different membership planes using Zadeh's S-function [51] with varying cross-over point. Among them, the one having minimal spatial and intensity fuzziness measured by entropy, index of fuzziness, or compactness measure, is regarded as the fuzzy segmented version of the image.

The second step is a construction of a skeleton membership plane; each pixel is assigned

a membership to the core-line, by considering three factors. The skeletal pixels should have high intensity, and they should occupy vertically and horizontally middle positions from the edges of the object, determined as the border of a support of a fuzzy segmented object. Suggestions how to define each membership term, and also how to combine them, are given. Either it is required that the pixel "highly" fulfils at least two out of three criteria, or some weighted sum of the criteria is calculated. In any case, membership values decrease at positions away from the core-line, and towards the edges of the object.

The third step is to generate α-cuts of the skeleton membership function, in order to determine the optimal skeleton (in terms of minimizing ambiguity in geometry or in the spatial domain). That is achieved by minimizing a (crisp) compactness measure, here defined as the ratio of the area and squared perimeter of the fuzzy object. With an increase of α, the compactness measure of the skeleton decreases, since less points are considered at each step, and both area and perimeter decrease. After achieving its optimum, the compactness measure increases again, since the object becomes disconnected, and the perimeter decreases more rapidly than the area. The α-cut providing minimal compactness for a skeleton is used in the process of enhancement and fuzzy segmentation, similarly as in the first step, for the initial membership function.

An approach which is theoretically interesting, but practically less useful, is presented in [29]. The method is called FMAT, and is a natural generalization of the MAT. It is defined by using either fuzzy disks, or convex fuzzy disks, but the FMAT of the image sometimes requires more storage space than specifying the original grey-scale image itself.

For any metric, a fuzzy disk centered at the point P is a fuzzy set in which membership values depend only on the distances from P. In [29], a fuzzy disk g_P^f in a fuzzy set f, having the center at P, is defined by

$$g_P^f(Q) = \inf_{d(P,R)=d(P,Q)} f(R),$$

for a metric d. Thus, g_P^f is the maximal fuzzy disk centered at P and not exceeding f. The set D_f of disk centres being local maxima of f (points having no neighbours Q such that $g_P^f < g_Q^f$), is the fuzzy medial axis of f, and $\{g_P^f \mid P \in D_f\}$ is the fuzzy medial axis transformation of f. This set is sufficient to reconstruct f, since it holds that

$$\sup_{P \in D_f} g_P^f = f.$$

It should be mentioned that fuzzy disks are not necessarily convex. If Euclidean metric is used, and f is fuzzy convex, then the g_P^f are fuzzy convex.

For an $n \times n$ digital image, and a chessboard distance, the total number of values needed to specify the FMAT is $\mathcal{O}(n^2)$.

In a grey-level image, the regions with locally higher grey-values can be understood in the global context as a set of lines which gives sufficient evidence for a perceptually meaningful sketch of an image, see Figure 14. Intuitively, the pattern can be interpreted as a Digital Elevation Model, and the identification of the skeleton on it can be related to

the detection of topographical features such as ridges, peaks and saddles. Detection of the skeleton of the pattern, by referring to the structural properties of its distance transform, is presented in [2]. An advantage of using a distance transform in the skeletonization process is that it creates a structure in the interior of the pattern, and guides the detection of the skeletal pixels in a more robust way, particularly regarding the extraction of the skeleton end-points.

In the case of binary images, the distance transform shows the way in which the background propagates over the pattern, and highlights the zones where interaction occurs between wave fronts coming from distinct parts of the background. However, in grey-level images, the length of a path, taking into account both spatial and intensity information, can be the same for different points, some of them not being positioned along the middle line of the image at all. To overcome this difficulty, structural information characterizing the distance transform of a single-valued region and information about dominance relations among the regions in the image are considered.

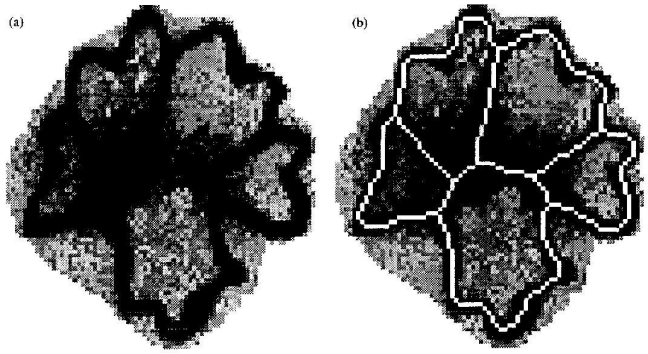

Figure 14: (a) A grey-tone pattern. (b) The skeleton obtained by using the procedure discribed in [2] (from [2]).

The pattern is seen as piecewise constant, and for each region with a constant grey-level the distance transform, based on the city-block distance, is computed. In particular, the distance between two neighbouring points is calculated as

$$L(p,q) = d(p,q) + |g(p) - g(q)|,$$

where $d(p,q) = 1$ is a spatial distance (distance in the xy-Cartesian plane) between p and q.

The constant-valued regions are classified into three groups, according to the grey-levels of the adjecent regions. Regions of first type are those where all adjacent regions have smaller grey-values. Within such regions the distance transform is unconstrained. All points belonging to them are certainly included into the skeleton.

Regions of the second type are those having both lower- and higher-valued neighbours. Within them the distance transform is constrained, with respect to the higher-valued region.

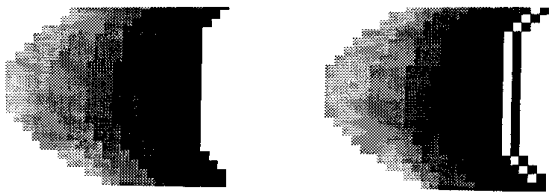

Figure 15: The skeleton is not found along the midline of the silhouette of the grey-tone pattern, but along the midline of the higher intensity region. (Left) Input. (Right) The skeleton (from [2]).

Regions of the third type are those having only higher grey-level neighbours. The distance transform within them is not computed, since the reference set (the set containing the points with lower grey-values) is empty. Such regions are hollows in the image. If the depth of a hollow is significant enough

(which is decided by some threshold), the skeleton contains a loop around it, since the region is seen as a part of the background. Otherwise, it is filled in, and merged with the neighbouring regions.

In a similar way, the number of significant plateaux (regions with high intensity) is reduced by merging neighbouring ones, if the difference between their grey-levels is lower than a predefined threshold.

Neighbourhood conditions, extending the ones which are valid in the binary case, are used to detect the set of intrinsic skeletal pixels on the Distance Transform, and to grow monotonously increasing paths to connect some of those pixels having locally higher distance labels. The conditions favour the detection of skeleton branches mainly along the central line of a region, they particularly prevent the creation of peripheral branches. Standard sequential removal operations are applied to obtain a one-pixel thick skeleton. In the end, two kinds of pruning, related to significance in terms of degree of elongation and in terms of grey-values, are done. The obtained set is reduced to unit width, and the pruning process is applied, in order to obtain a skeleton of a grey-tone pattern. An example is shown in Figure 15.

The presented procedure requires a number of input parameters (for the detection of significant plateaux, and hollows, and for pruning), whose values depend on the problem domain. Some questions about connectedness properties, as well as the type of distance transform which is used, are still open.

The skeletonization algorithm presented in [19] is based on the global properties of the boundary and skeleton curves. It is noticed that each skeletal point corresponds to at least

two boundary points – those where the maximal disk centered at the observed skeletal point touches the boundary. The distances from a skeletal point to both boundary points are equal. If the boundary is segmented into small segments, and the distance map from each of these segments is determined, the skeleton is located at the positions where at least two distance maps share the same value. These locations are identified as zero sets of distance map differences.

In order to determine the most appropriate way to segment the boundary, it is shown that a skeletal point is never generated by a single curve segment defined between successive positive curvature maxima. It is suggested to segment the shape boundary at points of positive maximal curvature, since in that case points generating the skeleton of a shape always belong to different boundary segments. For the segmentation of a closed curve, at least two partitioning points need to be assigned.

The algorithm consists of four main steps, as illustrated in Figure 16:

- find the curvature along the boundary curve and split the boundary into segments at the points of maximal positive curvature;
- for each segment calculate the Euclidean distance map over the whole image domain;
- find a preliminary skeleton as the location of the zero-level sets of all distance map differences;
- eliminate all background points and all points located on branches being too close to the corresponding boundary segment (at the distance lower that the reciprocal value of a curvature at the observed point).

The skeletonization algorithm described above can be successfully applied to all shapes unless they contain a specially shaped hole; in that case, the boundary of the hole (being a part of a shape boundary) does not necessarily contain two points of the negative curvature minima.

When applied to a discrete grey-level shape, the skeletonization algorithm includes interpolation of the boundary curve and its corresponding curvature. The discrete boundary of the object is obtained by subtracting a given threshold from an initial image, and taking the zero level of the resulting image. Distance maps are calculated on the grey-level images, by using numerical approximations which are consistent with the continuous case, so the method does not suffer from digitization bias, caused by a metrication errors and implementation on the grid.

A skeleton of a fuzzy shape can be computed by using fWDT, as presented in [10]. As in the binary case, the algorithm is based on iterative thinning guided by a distance transform. After calculating fWDT, the centres of maximal disks are detected. In this step, the points having labels lower than one half of a length of a of a horizontal step are considered as background points if they have at least one neighbour in the background, and kept (at least temporarily) if being surrounded by pixels with higher labels, to avoid creating spurious holes. All other labels are treated in the same way as in the classical

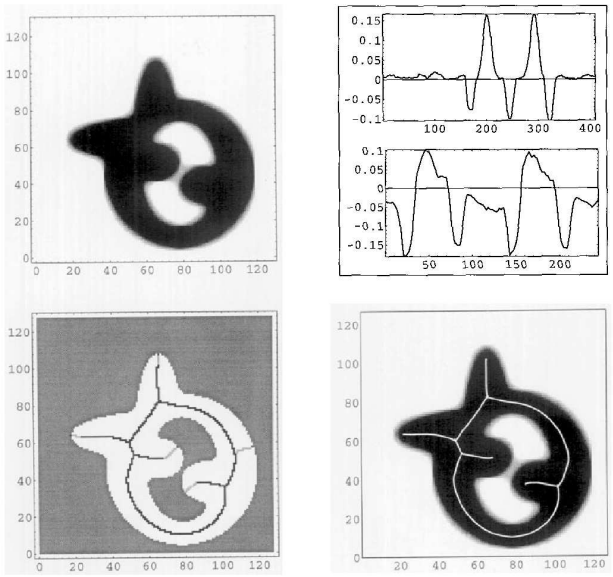

Figure 16: (Upper left) An object after geometric smoothing. (Upper right) Interpolated curvature function along the outer boundary (upper graph) and inner boundary (lower graph). (Lower left) Voronoi diagram of the segments (preliminary skeleton) in which the branches to be pruned are in light gray. (Lower right) The skeleton is the white curve, interpolated to subpixel accuracy, shown on the object (from [19]).

skeletonization algorithm, based on DT. The resulting skeleton is centered within the object with respect to the used fWDT. The topology of the object is preserved. The skeleton generated by using fWDT is, in general, smoother, compared to the one obtained by using WDT.

In Figure 17, first from the left, a cross section of a wood fibre in a scanning electron microscope image of paper is shown. The grey-levels of the pixels are in the range from 39 to 98. This is an example where the segmentation into object, fibre wall, and background is, in principle, easy. In Figure 18, the grey-level histogram for the image is shown. The peak for the object is centred around grey-level 56 and the peak for the background around grey-level 74. If the grey-levels are assumed to be normally distributed for both the object and the background, there is only a small overlap. Here, $T_l = 61$ (lower values are background), $T_h = 72$ (higher values are object), and pixels with grey-level 62 to 71 can be either object or background.

If we use a hard threshold and consider pixels with grey-level not lower than 62 as object, the resulting object (grey) and its skeleton (black) are shown in Figure 17, second from left. There are many non-significant skeleton components, and there is a bridge between the central fibre and the one at bottom right. If the threshold is set to 71, we get

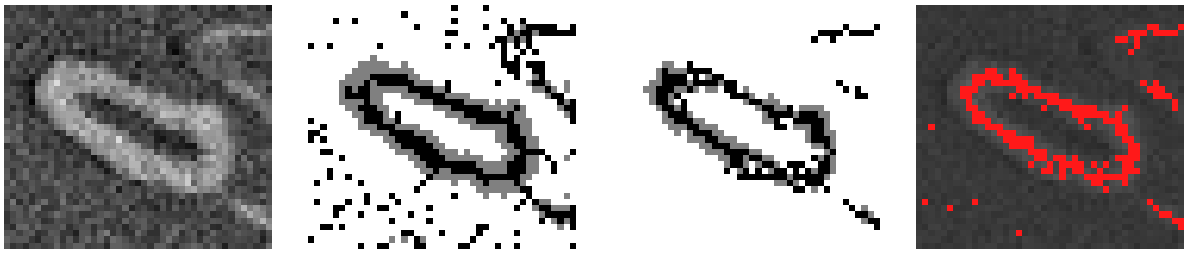

Figure 17: Grey-level image (first to the left) and skeletons resulting after using thresholds 62 (second to the left), 71 (third from the left), and the fuzzy border approach (the most right) (from [10]).

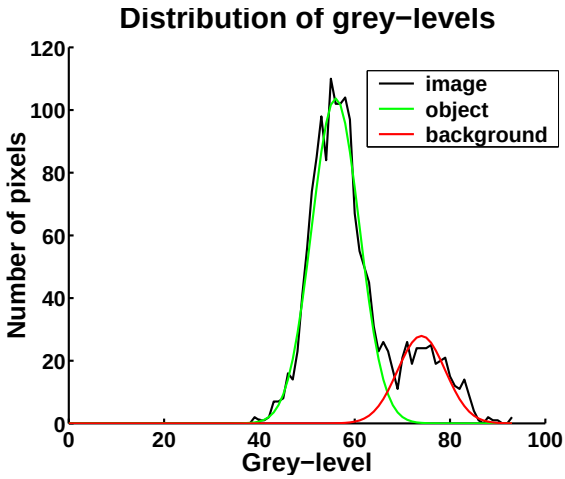

Figure 18: Grey-level histogram of Figure 17, left (from [10].

the skeleton in Figure 17, second from right. There are now holes in the skeleton, that do not correspond to holes in the fibre. If instead fWDT (here $\langle 5, 7 \rangle_{2D}$) and the described skeletonization algorithm is used, the resulting skeleton reflects the shape and topology for the imaged object in a better way, see Figure 17, right, where the skeleton consists of the points with the highest grey-level. This result has been achieved even though the grey-levels in the "bridge" between the fibres are the same as the ones in the "holes" in the fibre. The fWDT skeleton is also generally smother than the WDT one, even if this is hard to see in this small example.

A medial surface representation of a 3D grey-volume image is computed in [43]. The method combines distance information with grey-level information.

The suggested procedure reduces the foreground to a subset having the same topology as the initial foreground, constituted by surfaces (and curves) mainly placed along the

central position of the regions with locally higher intensity.

The first step is to compute the DT of all regions in the image. The voxels with grey-level g_k are labeled with the distance to their closest voxel in the reference set. Voxels placed in cavities are not reached by the distance propagation. After computation of the DTs, the voxels placed in cavities are set to the background level g_0.

The distance label assigned to a voxel can be interpreted as the iteration during erosion at which that voxel belongs to the border of the current foreground. Thus, an iterative thinning of the foreground, guided by the DT to identify the voxels that at each iteration constitute the border of the current foreground, is performed. To simplify the structure of the surface skeleton, some of its peripheral surfaces are removed to obtain the desired grey-medial surface representation.

6 Comments and conclusions

The fuzzy set theory has found a promising field of application in digital image processing. The use of fuzzy approaches for representing spatial relationships allows us to integrate both quantitative and qualitative knowledge about them, using the semi-quantitative interpretation of fuzzy sets. Fuzzy sets fit our intuitive knowledge of the diffuse localization or limits of the image components due to both uncertainty and imprecision.

Fuzziness is an intrinsic quality of images and a natural outcome of most picture processing techniques [6]. Two kinds of fuzziness can be distinguished, related to images. The first deals with crisp objects whose observation is corrupted by noise. Thus, fuzziness represents the imprecision and uncertainty due to noise. On the other hand, imprecision may be inherent to the observed objects and to the images, which leads to the second kind of fuzziness, that cannot be modeled by noise combined with a crisp object. The first type of fuzziness is not desired, and is preferably eliminated (if possible) before the analysis procedures, after which classical binary image analysis techniques can be performed. The second type provides important information, and is an essential part of the image [45, 6]. It has been shown to be useful to perform analysis while keeping this type of fuzziness present in the image as long as possible. Consequently, new appropriate image analysis methods are required.

The interest for developing such methods appeared almost forty years ago, and has been more or less active since then. That has resulted in the fuzzy shape analysis tool-box containing the extensions of almost all classical shape analysis methods, but with varying quality. While some of them, like distance transforms, and mathematical morphology, are rather intensively studied and well developed, some other, like moment-based methods, are hardly even mentioned in the literature. There are still a lot of challenges in fuzzy shape analysis; an evident improvement of the analysis, first of all in terms of precision and robustness, if fuzzy shape representations are used, seems to be a good motivation to take them.

References

[1] N. Ahuja, L. Davis, D. Milgram, and A. Rosenfeld. Piecewise approximation of pictures using maximal neighbourhoods. *IEEE Trans. Comput.*, C-27:375–379, 1978.

[2] C. Arcelli and G. Ramella. Sketching a grey-tone pattern from its distance transform. *Pattern Recognition*, 29:2033–2045, 1996.

[3] B. Biswas, A. Konar, and A. K. Mukherjee. Image matching with fuzzy moment descriptor. *Engineering Applications of Artificial Intelligence*, 14:43–49, 2001.

[4] I. Bloch. On fuzzy distances and their use in image processing under imprecision. *Pattern Recognition*, 32:1873–1895, 1999.

[5] I. Bloch. Geodesic balls in a fuzzy set and fuzzy geodesic mathematical morphology. *Pattern Recognition*, 33:897–905, 2000.

[6] I. Bloch and H. Maître. Fuzzy mathematical morphologies: A comparative study. *Pattern Recognition*, 28(9):1341–1387, 1995.

[7] H. Blum. A transformation for extracting new descriptors of shape. In W. Dunn, editor, *Models for the Perception of Speech and Visual Form*, pages 362–380, Cambridge MA, 1967. MIT Press.

[8] A. Bogomolny. On the perimeter and area of fuzzy sets. *Fuzzy Sets and Systems*, 23:257–269, 1987.

[9] G. Borgefors. Distance transformations in digital images. *Computer Vision, Graphics, and Image Processing*, 34:344–371, 1986.

[10] G. Borgefors and S. Svensson. Fuzzy border distance transforms and their use in 2D skeletonization. In R. Kasturi, D. Laurendeau, and C. Suen, editors, *Proceedings of International Conference on Pattern Recognition (ICPR 2002)*, volume I, pages 180–183. IEEE Computer Society, August 2002.

[11] J. Buckley and E. Eslami. Fuzzy plane geometry I: Points and lines. *Fuzzy Sets and Systems*, 86:179–187, 1997.

[12] J. Chanussot, I. Nyström, and N. Sladoje. Shape signatures of fuzzy sets based on distance from the centroide. *Pattern Recognition Letters*. To appear.

[13] B. Chaudhuri. Fuzzy convex hull determination in 2D space. *Pattern Recognition Letters*, 12:591–594, 1991.

[14] B. Chaudhuri. Some shape definitions in fuzzy geometry of space. *Pattern Recognition Letters*, 12:531–535, 1991.

[15] P. Diamond. A note on fuzzy starshaped fuzzy sets. *Fuzzy Sets and Systems*, 37:193–199, 1990.

[16] D. Dubois and M.-C. Jaulent. A general approach to parameter evaluation in fuzzy digital pictures. *Pattern Recognition Letters*, 6:251–259, 1987.

[17] H. Fonga. Pattern recognition in grey-level images by Fourier analysis. *Pattern Recognition Letters*, 17:1477–1489, 1996.

[18] L. Ikonen and P. Toivanen. Shortest route on height map using grey-level distance transforms. In I. Nyström, G. Sanniti di Baja, and S. Svensson, editors, *Proceedings of Discrete Geometry for Computer Imagery (DGCI 2003)*, volume 2886 of *LNCS*, pages 308–316, Naples, Italy, 2003. Springer-Verlag.

[19] R. Kimmel, D. Shaked, N. Kiryati, and A. Bruckstein. Skeletonization via distance maps and level sets. *Computer Vision and Image Understanding*, 62(3):382–391, 1995.

[20] G. Levi and U. Montanari. A grey-weighted skeleton. *Information and Control*, 17:62–91, 1970.

[21] S. Lončarić. A survey of shape analysis technique. *Pattern Recognition*, 31(8):983–1001, 1998.

[22] M. Maccarone. Fuzzy mathematical morphology: Concepts and applications. *Vistas in Astronomy*, 40(4):469–477, 1996.

[23] M. Machtegael and E. Kerre. Connections between binary, grey-scale and fuzzy mathematical morphologies. *Fuzzy Sets and Systems*, 124:73–85, 2001.

[24] G. Matheron. *Random Sets and Integral Geometry*, chapter xxiii, pp.261. John Wiley & Sons., New York, 1975.

[25] U. Montanari. A method for obtaining skeletons using a quasi-euclidean distance. *J. Assoc. Comput. Mach.*, 15(4):600–624, 1968.

[26] I. Nyström, G. Borgefors, and G. Sanniti di Baja. 2D grey-level convex hull computation: A discrete 3D approach. In J. Bigun and T. Gustavsson, editors, *Proceedings of* 13^{th} *Scandinavian Conference on Image Analysis (SCIA 2003)*, volume 2749 of *LNCS*, pages 763–770, Göteborg, Sweden, 2003. Springer-Verlag.

[27] S. Pal. Fuzzy skeletonization of an image. *Pattern Recognition Letters*, 10:17–23, 1989.

[28] S. Pal and A. Rosenfeld. Image enhancement and thresholding by optimization of fuzzy compactness. *Pattern Recognition Letters*, 7:77–86, 1988.

[29] S. Pal and A. Rosenfeld. A fuzzy medial axis transformation based on fuzzy disks. *Pattern Recognition Letters*, 12:585–590, 1991.

[30] F. Pasian and C. Vuerli. Core-line tracing for fuzzy image subsets. *Pattern Recognition Letters*, 4:93–98, 1986.

[31] S. Peleg and A. Rosenfeld. A min-max medial axis transformation. *IEEE Trans. on Pattern Analysis and Machine Intelligence*, PAMI-3(2):208–210, 1981.

[32] A. T. Popov. Convexity indicators based on fuzzy morphology. *Pattern Recognition Letters*, 18:259–267, 1997.

[33] A. Rosenfeld. Fuzzy digital topology. *Information and Control*, 40:76–87, 1979.

[34] A. Rosenfeld. The diameter of a fuzzy set. *Fuzzy Sets and Systems*, 13:241–246, 1984.

[35] A. Rosenfeld. The fuzzy geometry of image subsets. *Pattern Recognition Letters*, 2:311–317, 1984.

[36] A. Rosenfeld and S. Haber. The perimeter of a fuzzy subset. *Pattern Recognition*, 18:125–130, 1985.

[37] P. K. Saha, F. W. Wehrli, and B. R. Gomberg. Fuzzy distance transform: Theory, algorithms, and applications. *Computer Vision and Image Understanding*, 86:171–190, 2002.

[38] J. Serra. *Image Analysis and Mathematical Morphology, Part II: Theoretical Advances*. Academic Press, London, 1988.

[39] D. Sinha and E. Dougherty. Fuzzification of set inclusion, theory and application. *Fuzzy Sets and Systems*, 55:15–42, 1993.

[40] N. Sladoje. Reviews of scientific papers on fuzzy set theory in image segmentation. Internal Report 24, Centre for Image Analysis, Uppsala, Sweden, 2002.

[41] N. Sladoje, I. Nyström, and P. Saha. Perimeter and area estimations of digitized objects with fuzzy borders. In I. Nyström, G. Sanniti di Baja, and S. Svensson, editors, *Proceedings of Discrete Geometry for Computer Imagery (DGCI 2003)*, volume 2886 of *LNCS*, pages 368–377, Naples, Italy, 2003. Springer-Verlag.

[42] C. Sun. Symmetry detection using gradient information. *Pattern Recognition Letters*, 16:987–996, 1995.

[43] S. Svensson, I. Nyström, C. Arcelli, and G. Sanniti di Baja. Using grey-level and distance information for medial surface representation of volume images. In R. Kasturi, D. Laurendeau, and C. Suen, editors, *Proceedings of International Conference on Pattern Recognition (ICPR 2002)*, volume II, pages 324–327. IEEE Computer Society, august 2002.

[44] P. Toivanen. New geodesic distance transforms for grey-scale images. *Pattern Recognition Letters*, 17:437–450, 1996.

[45] J. K. Udupa and S. Samarasekera. Fuzzy connectedness and object definition: Theory, algorithms, and applications in image segmentation. *Graphical Models and Image Processing*, 58(3):246–261, May 1996.

[46] T. Wakayama. A core-line tracing algorithm based on maximal square moving. *IEEE Trans. on Pattern Analysis and Machine Intelligence*, PAMI-4:68–74, 1982.

[47] S. Wang, A. Rosenfeld, and A. Wu. Image approximation from grey scale "Medial Axis". *IEEE Trans. on Pattern Analysis and Machine Intelligence*, PAMI-3(6):687–696, 1981.

[48] S. Wang, A. Rosenfeld, and A. Wu. A medial axis transformation for grayscale pictures. *IEEE Trans. on Pattern Analysis and Machine Intelligence*, PAMI-4(4):419–421, 1982.

[49] X. Yuan and Z. Shen. Notes on "Fuzzy plane geometry I, II". *Fuzzy Sets and Systems*, 121:545–547, 2001.

[50] L. Zadeh. Fuzzy sets. *Information and Control*, 8:338–353, 1965.

[51] L. Zadeh. Calulus of fuzzy restrictions. In L. Z. et al., editor, *Fuzzy Sets and their Application to Cognitive and Decision Processes*, pages 1–39, London, 1975. Academic Press.

[52] M. Zribi. Description of three-dimensional grey-level objects by the harmonic analysis approach. *Pattern Recognition Letters*, 23:235–243, 2002.